Konstantin Eduardovich Plokhotnikov

Mathematical Model of Geopolitics

SOCIETY FOR SCIENCE AND EDUCATION

Mathematical Model of Geopolitics

By: Konstantin Eduardovich Plokhotnikov

CONTENTS

ABSTRACT

The mathematical model of geopolitics is a conditional name for several models, which are naturally connected and act as accompaniment to the main theme — geopolitics. All constructed work models made the transition to computing experiment, the results of which are given and discussed. The central concept of the mathematical model of geopolitics is introduced — the capacity of the habitat. Geopolitics is the climate, the relief, the logistics features of global commodity flows, the geopolitical confrontation in terms of the "sea-continent", i.e. all that constitutes the material complex of living conditions of the inhabitants of the Earth. This complex, to a large extent, mediates the population's behavior from the political point of view. The author does not adhere to the position of natural determinism, which acts in the form of geopolitics, but tries to delineate the scope of the manifestation of geopolitics in real politics. The paper provides clarification and generalization of the generally accepted geopolitical classification of territories in terms of orientation and positioning either at sea or on the continent. The mathematical model of transport costs minimization for an arbitrary number of points acting in the form of logistic centers is formulated.

Keywords: the capacity of the habitat, the average annual temperature and moisture, relief, correlation analysis, cutting territories, the geopolitical classification of points (territories), traffic, nonlinear optimization.

E-mail: psygma@yandex.ru

Affiliation: Lomonosov Moscow State University, Financial University under the Government of the Russian Federation

INTRODUCTION

In a number of works by the author [1, 2] the “Normative model of global history” was formulated. At the heart of this model lies the representation of global political integrity as a set of atomic units, called geopatom (GEOPolitical ATOMs). It seems that the current political structure of the territories of human habitation on Earth, to a large extent, can be explained by combining a specially prepared smaller territories — geopatoms. In connection with this hypothesis there is the task of building a set of geopatoms, covering the entire territory of the Earth.

For adequate cutting of the Earth's territory into individual geopatoms, it is necessary to take into account the climatic features of the territories, as well as the relief. In addition, it is also necessary to take into account global traffic, which significantly changes the configuration of the location and shape of the geopatoms.

To take into account for climatic peculiarities of living in these territories the concept of “capacity of the habitat” will be formulated. Will be built a suitable density function of the capacity of the habitat, which will include the whole complex of anthropomorphic requirements to the environment in terms of climate. The areas of residence of people will be classified in terms of “(not) highly – (not) favorable”, i.e. taking into account height above sea level and climatic features.

In terms of global traffic modelling, the central geopolitical confrontation between the “sea” and the “continent” will be particularly acute, as warned by the classics of geopolitics. The formulation of the algorithm and the calculation of global traffic flows with its help will clarify and summarize the classification of all territories in the conventional geopolitical categories.

SECTION I.
THE CAPACITY OF THE HABITAT

We will construct a mathematical model of what is called differently in different disciplines: the capacity of the habitat, the living space etc. We will be interested in the construction of the measure of the volume the capacity of the habitat by taking into account various kinds of the most important natural components that accompany people's lives. Such components include, primarily, the annual averages of temperature and precipitation on the Earth's surface.

A spatial scan in the model bind with latitude φ and longitude λ of the Earth's surface, considering that $\varphi\in[-\pi/2,\pi/2]$, $\lambda\in[-\pi,\pi]$ — in radians or $\varphi\in[-90^0,90^0]$, $\lambda\in[-180^0,180^0]$ — in degrees. To select a suitable formula for the connection of the density of the capacity of the habitat, ρ with the average annual temperature T_{annual} and the precipitation Q_{annual} we draw real data available for the entire surface of the Earth.

We introduce comfortable temperatures from the point of view of people's living, T_{comfort} and precipitation, Q_{comfort} according to the weighted average procedure, choosing the density of people's living on the surface of the Earth as a weight, p_{density}. In this case, we can write down the following general formula for calculating T_{comfort} and Q_{comfort}:

$$T_{\text{comfort}}=\frac{\iint T_{\text{annual}}p_{\text{density}}\cos\varphi d\varphi d\lambda}{\iint p_{\text{density}}\cos\varphi d\varphi d\lambda}, Q_{\text{comfort}}=\frac{\iint Q_{\text{annual}}p_{\text{density}}\cos\varphi d\varphi d\lambda}{\iint p_{\text{density}}\cos\varphi d\varphi d\lambda}, (1)$$

where $T_{\text{annual}}=T_{\text{annual}}(\varphi,\lambda)$, $Q_{\text{annual}}=Q_{\text{annual}}(\varphi,\lambda)$, $p_{\text{density}}=p_{\text{density}}(\varphi,\lambda)$ — corresponding latitude and longitude functions. The integration in (1) is assumed throughout the globe without taking into account the water surface.

Let's choose a spatial resolution of $0{,}5^0$ degrees and consider the specific data for the average annual temperature, precipitation and population density. In this case, the data will appear in the form of matrices of size 360×720, where 360 is the number of nodes of a uniform grid in latitude and 720 — longitude. Grids in latitude and longitude in radians can be represented as $\varphi_i=\frac{\pi}{180}[-89{,}75+0{,}5(i-1)], i=1,\dots,360;$ $\lambda_j=\frac{\pi}{180}[-179{,}75+0{,}5(j-1)], j=1{,}2,\dots,720.$

Load the data on annual average temperature and precipitation from the site [3]. We choose the version of archive 2.02, which is dated July 2001. A description of the archive data is available on the website [4]. Data on the density of the population of the Earth we take from the site NASA Earth Observations [5].

Replace the integration in (1) by summation over our grid, then

$$T_{\text{comfort}}\cong\frac{\sum_{i,j}T_{\text{annual},i,j}p_{\text{density},i,j}\cos\varphi_i}{\sum_{i,j}p_{\text{density},i,j}\cos\varphi_i}, Q_{\text{comfort}}\cong\frac{\sum_{i,j}Q_{\text{annual},i,j}p_{\text{density},i,j}\cos\varphi_i}{\sum_{i,j}p_{\text{density},i,j}\cos\varphi_i}, \qquad (2)$$

where the summation in (2) is carried out over those grid nodes that do not belong to the water surface.

According to the formula (2) the calculation was carried out with data from the archive 2.02 and NASA data on population density, it was found that $T_{\text{comfort}} = 18{,}5775^0C$; $Q_{\text{comfort}} = 1200{,}2$ mm.

The weighted average standard deviations from comfort values were also calculated, they turned out to be equal to $T_{\text{comfort,std}} = 7{,}9084^0C$ and $Q_{\text{comfort,std}} = 722{,}5299$ mm respectively for temperature and precipitation. Such noticeable standard deviations indicate that the proposed dependence of the capacitance of the medium ρ from deviations from the comfort values in the form of power expressions such $|T/T_{\text{comfort}} - 1|^{\alpha}$ and $|Q/Q_{\text{comfort}} - 1|^{\beta}$ should be small compared with 1 values of degrees α and β.

After entering comfort values of temperature and precipitation, we choose for further analysis the following formula for describing the density of capacity of the habitat:

$$\rho = \rho(T, Q) = e^{a_1 + a_2|T/T_{\text{comfort}} - 1|^{\alpha} + a_3|Q/Q_{\text{comfort}} - 1|^{\beta}}, \qquad (3)$$

where $a_1, a_2, a_3, \alpha, \beta$ — while undefined constant.

In the representation (3) the entire set of requirements for the function ρ is focused. The function describing the capacity of the medium[1], ρ must be nonnegative, depend on deviations from comfort values that are easily modified if an additional parameter describing the capacity of the medium is taken into account.

The uncertain parameters a_1, a_2, a_3 entering in (3) are found by minimizing the sum of squares of deviations of the inverse function of the medium's capacity, $1/\rho$ from the inverse population density function, $1/p_{\text{density}}$. It turned out, that precisely in this case the correlation between the inverse of the capacity of the medium and the inverse of the population density, $s_{\text{density}} = 1/p_{\text{density}}$ is maximized. The value of the s_{density} has a clear geographical sense — it is the number of square kilometers per person in the region, if the p_{density} is measured in the number of people per square kilometer.

Taking into account (1), we write down a functional D whose minimum provides a search for the parameters a_1, a_2, a_3 for fixed values of α, β:

$$D = D(a_1, a_2, a_3) = \frac{\iint [\rho^{-1}(\varphi,\lambda) - p_{\text{density}}^{-1}]^2 \cos\varphi d\varphi d\lambda}{\iint \cos\varphi d\varphi d\lambda} \longrightarrow \min_{a_1, a_2, a_3} D, \qquad (4)$$

where integration is assumed over the entire land, without taking into account the water surface.

[1] Means the same as “the capacity of the habitat” or “the capacity of environment”.

Taking (2) into account, we rewrite the functional (4) in finite-difference form, proceeding, as above, from the resolution of $0{,}5^0$. In this case, up to the numerical coefficient, we obtain

$$D = D(a_1, a_2, a_3) \cong \frac{1}{N}\sum_{i,j}[\rho_{i,j}^{-1} - p_{\text{density},i,j}^{-1}]^2 \cos\varphi_i, \qquad (5)$$

where $i = 1, \dots, 360$; $j = 1, \dots, 720$; N — the number of grid nodes on the land surface, and the summation extends only to those grid nodes that fall on the land.

To find the minimum of the functional in the form of (5) the problem of gradient descent was solved

$$\frac{da_k}{dt} = -\frac{\partial D(a_1,a_2,a_3)}{\partial a_k}, k = 1,2,3, \qquad (6)$$

where t is some conditional argument, herewith

$$\frac{\partial D}{\partial a_1} = -\frac{2}{N}\sum_{i,j}\rho_{i,j}^{-1}(\rho_{i,j}^{-1} - p_{\text{density},i,j}^{-1})\cos\varphi_i,$$
$$\frac{\partial D}{\partial a_2} = -\frac{2}{N}\sum_{i,j}|T_{i,j}/T_{\text{comfort}} - 1|^{\alpha}\rho_{i,j}^{-1}(\rho_{i,j}^{-1} - p_{\text{density},i,j}^{-1})\cos\varphi_i,$$
$$\frac{\partial D}{\partial a_3} = -\frac{2}{N}\sum_{i,j}|Q_{i,j}/Q_{\text{comfort}} - 1|^{\beta}\rho_{i,j}^{-1}(\rho_{i,j}^{-1} - p_{\text{density},i,j}^{-1})\cos\varphi_i.$$

The system of differential equations (6) can be solved using one of the standard solvers, for example, the MATLAB package. The solution was carried out until the values a_1, a_2, a_3 were established, i.e. when it is possible to clearly identify the presence of the limits of the values a_1, a_2, a_3 for $t \to +\infty$.

Table 1. List of values of the parameters included in the formula for the capacity of the habitat

#	T_{comfort}	Q_{comfort}	a_1	a_2	a_3	α	β	Corr
1	18,5775	1200,2	0,7156	–0,0649	–0,0426	2	2	0,5758
2	18,5775	1200,2	1,0227	–0,2767	–0,2991	1	1	0,6329
3	18,5775	1200,2	1,6592	–0,6627	–0,6656	0,5	0,5	0,6581
4	18,5775	1200,2	6,2794	–3,2566	–2,7573	0,1	0,1	0,6590
5	18,5775	1200,2	3,4189	–1,6624	–1,4789	0,2	0,2	0,6611

Table 1 contains a list of the values of the parameters entering into the formula (3) for the medium capacity, obtained taking into account the solution of problems (2), (5), (6). In addition, Table 1 shows the corresponding values of the correlation coefficient, Corr, which establishes the relationship between the sets $\{\rho_{i,j}^{-1}\}$ and $\{p_{\text{density},i,j}^{-1}\}$, $i = 1, \dots, 360$; $j = 1, \dots, 720$. Taking into account the features of the geometry on the sphere, the correlation was calculated by the formula:

$$\text{Corr} = \frac{\frac{1}{N}\sum_{i,j}(\rho_{i,j}^{-1} - \overline{\rho^{-1}})(p_{\text{density},i,j}^{-1} - \overline{p_{\text{density}}^{-1}})\cos\varphi_i}{\sqrt{\frac{1}{N}\sum_{i,j}(\rho_{i,j}^{-1} - \overline{\rho^{-1}})^2\cos\varphi_i}\cdot\sqrt{\frac{1}{N}\sum_{i,j}(p_{\text{density},i,j}^{-1} - \overline{p_{\text{density}}^{-1}})^2\cos\varphi_i}}, \qquad (7)$$

where

$\overline{\rho^{-1}} = \frac{1}{N}\Sigma_{i,j}\,\rho_{i,j}^{-1}\cos\varphi_i,\ \overline{p_{\text{density}}^{-1}} = \frac{1}{N}\Sigma_{i,j}\,p_{\text{density},i,j}^{-1}\cos\varphi_i.$

Figure 1 shows typical samples of the dependence of the modulus of the gradient $G = \sqrt{\left(\frac{\partial D}{\partial a_1}\right)^2 + \left(\frac{\partial D}{\partial a_2}\right)^2 + \left(\frac{\partial D}{\partial a_3}\right)^2}$ and the value of the functional (5), D on the argument t. The graphs in Figure 1 demonstrate the obvious convergence of the modulus of the gradient G to zero (the left graph), and the value of the functional D to some limiting, minimum value (right graph). This means that the set of parameters a_1, a_2, a_3 converges to its limiting values when $t \to +\infty$. The other parameter values are chosen according to point #5 of the Table 1, when there was a maximum correlation value.

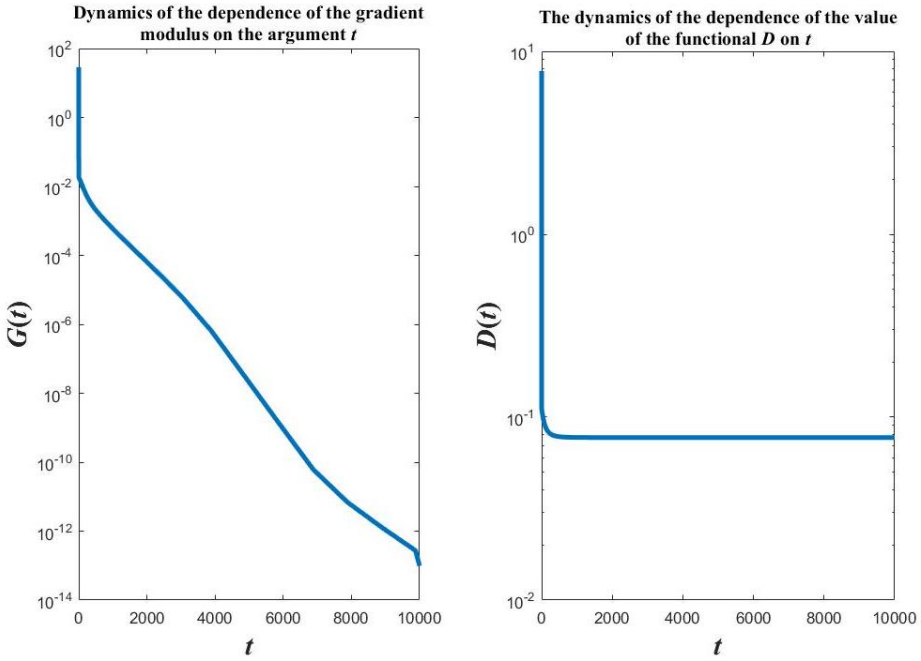

Figure 1. Dynamics of modulus gradient G (left graph) and the functional values D (right graph) on the argument t

The negative values of the signs of the parameters a_2, a_3 in Table 1 meet our expectations. The values of parameters α and β were subjected to variation. It was found that the maximum correlation value, excluding a small variation is in the neighborhood of values of degrees $\alpha = 0{,}2$ and $\beta = 0{,}2$. Note that if in the formula for the capacity of the medium (3) the precipitation is not taken into account ($a_3 = 0$), the correlation coefficient at the parameter value from point #5 of Table 1 will be 0,6341. The resulting value is slightly less than the number 0,6611, i.e. precipitation component provides its contribution. Finally, in the absence of temperature in formula (3) ($a_2 = 0$) the correlation value was 0,5587, which is noticeably less than 0,6611. These observations mean that the combined use of temperature and precipitation indicators increases the correlation between the values of the inverse capacity function of the habitat and the inverse function of population density.

Thus, it can be concluded that approximately two-thirds of the correlation between the inverse function of the habitat capacity calculated by formula (3) and the inverse population density function falls on the habitat in terms of temperature and precipitation.

Let us compare visually the maps of the inverse function of the density of the capacity of the habitat and the inverse function of the population density. The required maps will be drawn using level lines. Figure 2 shows the result. On the left map of Figure 2 shows the level line of the inverse function of the density of the medium's capacitance, calculated by the formula (3) with parameters from point #5 of the Table 1. In total, 12 level lines with equidistant values are constructed, which show the range of variation of the invers capacity [0,0054;1,1268]. On the right the map Figure 2 shows the inverse function of population density. Also constructed are 12 level lines with equidistant values, which represent the range of variation in the population inverse density [0,0001;0,9664].

In Figure 2 more blue up to violet flowers with small values of the inverse function of the density of the habitat capacity and inverse population density function are marked. There is a clear correlation between the locations of the blue and violet spots on the left and right maps of Figure 2. Note that these places meet the most comfortable place for human living conditions. There are significant differences on all continents. To the right of each of the maps is a palette that establishes a connection with the numerical value of the corresponding indicator. In addition, on each of the maps has a coastline in the form of a red line.

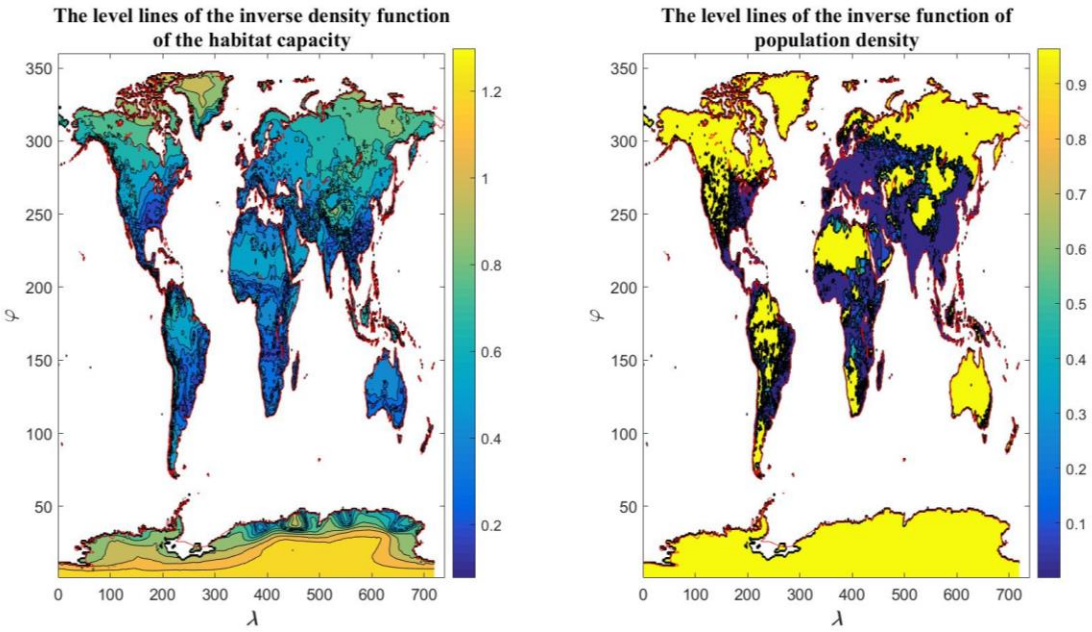

Figure 2. Maps of level lines of the inverse density function of the habitat capacity (left) and the inverse population density function (on the right)

Let's move from the inverse density values of the habitat capacity and density of population to the direct values. Compare the linear Pearson correlation coefficient and rank correlation Kendall and Spearman correlation for the density capacity of the habitat and

density of population. To do this, we transform the matrices $\rho_{i,j}\sqrt{\cos\varphi_i}$ and $p_{\text{density},i,j}\sqrt{\cos\varphi_i}$ into vectors and find the corresponding correlation coefficients between these vectors. Table 2 summarizes the results.

Table 2. The correlation coefficients of Pearson, Kendall, and Spearman between the density of habitat capacity and the population density

Correlation coefficient	Pearson	Kendall	Spearman
The value of the correlation coefficient	0,1740	0,7582	0,9034

Table 2 shows how large are the rank correlation coefficients compared with the conventional linear correlation coefficient. For this reason, in the formula (7) the linear correlation between the inverse density function of the capacity of the habitat and density of population was considered. For the inverse values, the linear correlation coefficient was found to be 0,6611, which is much larger than 0,1740.

As a result of the above constructions and calculations, we choose the function (3) for the function of the capacitance of the habitat of people, which reflects the relationship with such characteristics as temperature and precipitation, or more precisely, with deviations in temperature and precipitation from the corresponding comfort values.

SECTION II.
THE DISTRIBUTION CAPACITY OF HABITAT IN THE STATES

Taking into account the functional representation for the habitat capacity (3), we will write the formula for calculating the global capacity of the habitat:

$$U = \int_{-\pi/2}^{\pi/2} d\varphi \int_{-\pi}^{\pi} d\lambda \cos\varphi \cdot \rho(T(\varphi,\lambda), Q(\varphi,\lambda)). \quad (8)$$

In the beginning, we will find the center of concentration or the center of the scattering of the capacity of the habitat and compare it with the center of the dispersion of the population of the Earth. Let us turn to a discrete representation of all integral indicators, starting from a grid in latitude and longitude, the size of 360×720. We calculate the center of population dispersion according to formulas:

$$\varphi_{\text{population}} = \frac{\sum_{i,j} \varphi_i p_{\text{density},i,j} \cos\varphi_i}{\sum_{i,j} p_{\text{density},i,j} \cos\varphi_i}, \lambda_{\text{population}} = \frac{\sum_{i,j} \lambda_j p_{\text{density},i,j} \cos\varphi_i}{\sum_{i,j} p_{\text{density},i,j} \cos\varphi_i}, \quad (9)$$

where the summation extends to those pairs (φ_i, λ_j), $i = 1, \dots, 360$; $j = 1, \dots, 720$, that belong to the land. The population density of p_{dencity} will be the same as in the previous section.

Similarly to formulas (9), we define the expressions for calculating the scattering center of the capacity of the habitat:

$$\varphi_{\text{capacity}} = \frac{\sum_{i,j} \varphi_i \rho_{i,j} \cos\varphi_i}{\sum_{i,j} \rho_{i,j} \cos\varphi_i}, \lambda_{\text{capacity}} = \frac{\sum_{i,j} \lambda_j \rho_{i,j} \cos\varphi_i}{\sum_{i,j} \rho_{i,j} \cos\varphi_i}, \quad (10)$$

where $\rho_{i,j}$, $i = 1, \dots, 360$; $j = 1, \dots, 720$ is the density of the habitat capacity (3) with the values of the parameters from point #5 of Table 1.

Figure 3,a shows the total count of population dispersion centers, $(\varphi_{\text{population}}, \lambda_{\text{population}})$ and habitat capacity, $(\varphi_{\text{capacity}}, \lambda_{\text{capacity}})$. It turned out that the center of population dispersion has coordinates (23,78 N; 51,85 E) — Arabian Peninsula, Saudi Arabia, salines. The center for the dispersion of habitat capacity has coordinates (13,59 N; 19,03 E) — Central Africa, Central Chad, east of Ndjamena.

Note that in the model, both the dimension and the absolute value of the habitat capacity are not significant. Only the spatial sweep is important, i.e. the relative values of the capacity of the habitat or individual regions, or the density of the medium of individual points.

As an example of calculating the global capacity of the environment (8) let us consider the world political map with borders of individual States and territories and calculate the capacity of the habitat for each of the States and territories. According to the UN data for 2008, the borders of 246 States and territories, data on which are presented, for example,

on the website [6], are marked. Figure 3,b shows a graphic illustration of all the boundaries of states and territories available for 2008.

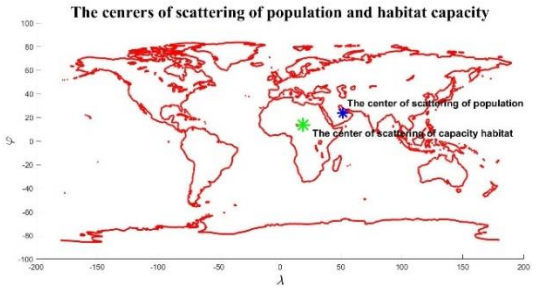

Figure 3,a. Population scattering centers (Arabian Peninsula), and the capacity of habitat (Central Africa)

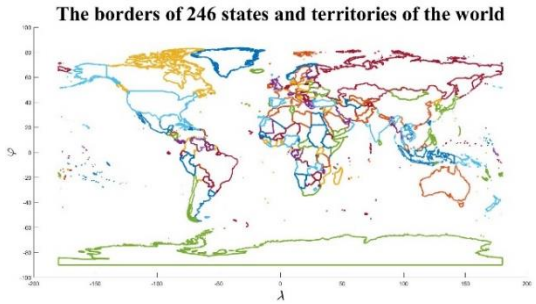

Figure 3,b. The borders of 246 states and territories of the world

Define the region occupied by the k-th State or territory, with the symbol ω_k. In this case, the global capacity of the habitat (8), taking into account the selected marking of the Earth's surface, can be rewritten as:

$$U = \sum_{k=1}^{246} u_k \,, u_k = \iint_{\omega_k} d\varphi d\lambda \cos\varphi \cdot \rho(T, Q). \qquad (11)$$

To calculate the capacity of the habitat of all States and territories u_k, $k = 1, \dots, 246$ we replace the double integrals in (11) with approximate sums, starting from a resolution of half a degree in latitude and longitude. In this case, the second equation in (11) can be rewritten in the form:

$$u_k \cong \left(\frac{\pi}{360}\right)^2 \sum_{\varphi_i, \lambda_j \in \omega_k} \cos\varphi_i \, \rho_{i,j}, \qquad (12)$$

where $i = 1, \dots 360$, $j = 1, \dots, 720$, and the summation in (12) extends to those points (φ_i, λ_j), that enter the region ω_k.

A computational experiment was carried out to calculate the set of capacities of the habitat of States and territories (12), while the matrix $\rho_{i,j}$ was calculated from formula (3) with parameters from point #5 of Table 1.

Figure 4 shows the final graph, which marked some countries and territories, deployed in terms of habitat capacity. In particular, the top five in terms of capacity of the habitat in descending order is as follows: Russia, the United States, Brazil, China, Australia with the values of 0,6027; 0,5818; 0,5261; 0,5061; 0,4968 respectively.

The global capacity of the habitat U was 7,6438, with an average value of — 0,0311, and a standard deviation of — 0,0863.

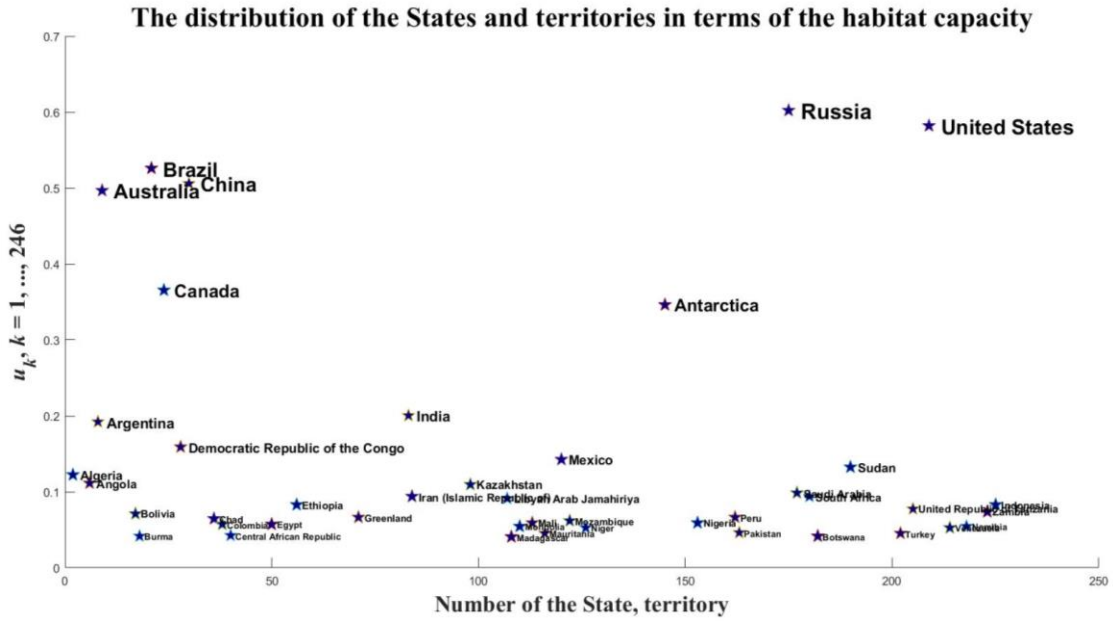

Figure 4. The distribution of the States and territories in terms of the habitat capacity

Let us study the distribution of the capacity of the habitat per person. We introduce a suitable variable in the following form:

$$v_k = u_k / p_{\text{population},k}, \qquad (13)$$

where $p_{\text{population},k}$ — population of the k-th State or territory, $k = 1, \dots, 246$.

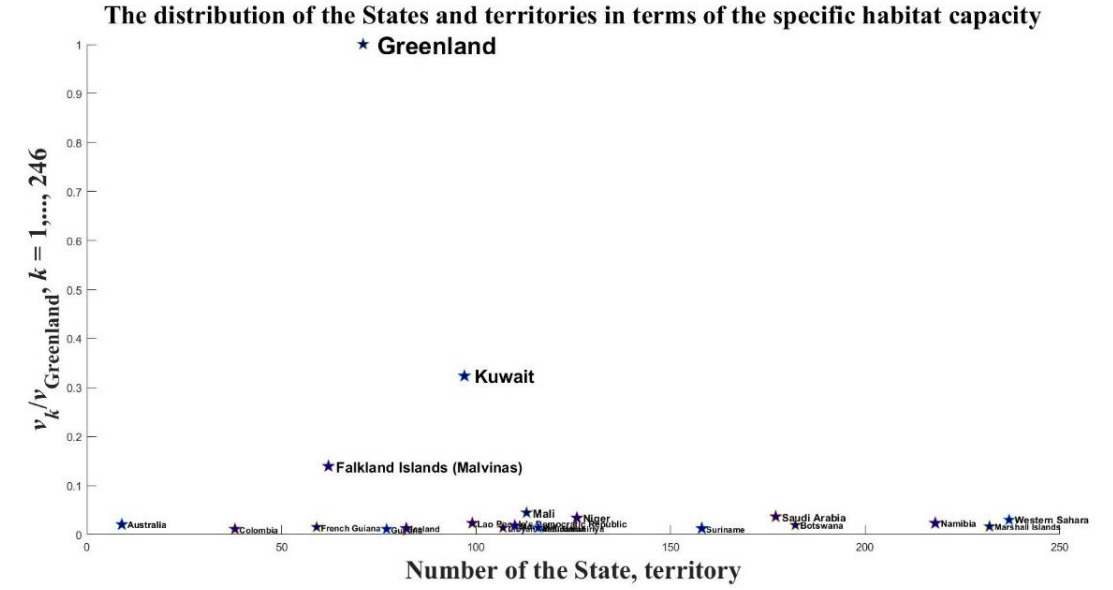

Figure 5. The distribution of the States and territories in terms of the specific habitat capacity

The variable v_k, introduced in (13), denotes the volume of the habitat per person within the k-th State or territory or the specific value of the volume of the habitat. As specific values of the population were selected data for 2005, which are given in the same data source as the data of the borders of 246 States and territories.

The performed calculation of the set of indicators v_k, $k = 1, \dots, 246$ showed that the winner is Greenland. Figure 5 shows a graph similar to that in Figure 4, where some values of the set of specific volumes of the medium v_k, $k = 1, \dots, 246$, normalized to the maximum specific volume $v_{\text{Greenland}}$, are plotted along the ordinate.

Table3. The ratio of the specific volume of the Russian habitat to the specific volumes of a number of other countries

Russia/Finland	Russia/United Kingdom	Russia/France	Russia/Germany
1,5416	17,6738	7,5665	16,6839
Russia/Poland	**Russia/Ukraine**	**Russia/Turkey**	**Russia/Kazakhstan**
10,4924	6,8427	6,7931	0,5802
Russia/China	**Russia/Japan**	**Russia/USA**	
10,8619	23,3693	2,1576	

Consider the ratio of the specific capacity of Russia's habitat in relation to a number of other States. Table 3 shows some characteristic list of relations.

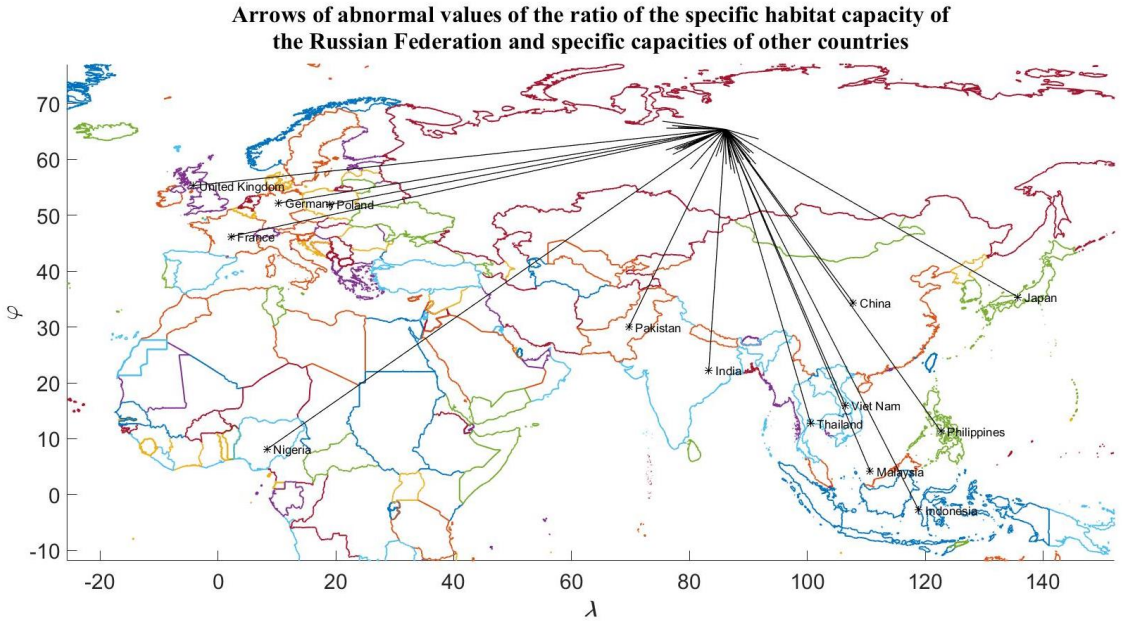

Figure 6. Arrows of abnormal values of the ratio of the specific habitat capacity of the Russian Federation and specific capacities of other countries

According to Table 3, the largest values of the ratio of the specific volume of the Russia habitat to the specific volumes of other countries fall on the three countries traditionally

included in the historical orbit of the Russian Federation: The United Kingdom, Germany and Japan.

We will construct a map on which the arrows indicate the transitions from those countries which, on the one hand, have a sufficiently high potential for the capacity of the habitat ($u_k > 0{,}02 \max\limits_{1 \le i \le 246} u_i$), on the other hand, the ratio of the specific habitat capacity of the Russian Federation to the specific capacity of another country is greater than a certain threshold value ($v_{\text{Russia}}/v_k > 7{,}5$). Thus, we take into account only those countries whose habitat capacity exceeds 2% of the capacity of the largest state, i.e. the Russian Federation. As the threshold value of the ratio of the specific habitat capacity of the Russian Federation and the specific capacities of other countries, we choose the value 7,5, that is, a sufficiently high value.

In Figure 6 shows a map with the desired arrows. With the selected thresholds for the capacities of the habitat and the specific capacities of individual countries, there were 13 arrows that oppose 13 countries with the Russian Federation. Part of the countries shown in Figure 6 also appear in Table 3. Note that all 13 arrows are directed to the Russian Federation.

SECTION III.
CAPACITY OF HABITAT (POPULATION DENSITY) AND RELIEF

Using the relevant data, we will study the density of the habitat capacity (population density) in connection with the relief of the Earth's surface[2]. The relief data is represented in latitude, longitude coordinates with a resolution of $0{,}5^0$ in the form of a matrix $Z_{i,j}$, $i = 1, \dots, 360$; $j = 1, \dots, 720$.

We define a set of average heights in different senses: the average height of the land, $\bar{Z}$; weighted average height, $\bar{Z}_{\text{population}}$, where the population density is chosen as the weight; as well as the average weighted population density of 50% of the population, $\bar{Z}_{\text{population},50\%}$, where $Z < Z_*$ and $p_{\text{density}} > p_*$, where Z_*, p_* — are some nonnegative constants. The averages listed above are found according to the following formulas:

$$\bar{Z} = \frac{\sum_{i,j} Z_{i,j} \cos\varphi_i}{\sum_{i,j} \cos\varphi_i},\ \bar{Z}_{\text{population}} = \frac{\sum_{i,j} Z_{i,j} p_{\text{density},i,j} \cos\varphi_i}{\sum_{i,j} p_{\text{density},i,j} \cos\varphi_i}. \qquad (14)$$

The formula for calculating $\bar{Z}_{\text{population},50\%}$ is similar to the second formula in (14), provided that the summation extends over those pairs of indices (i, j), for which the following inequalities are true: $Z_{i,j} < Z_*$ and $p_{\text{density},i,j} > p_*$. The threshold values Z_*, p_* were selected from those considerations that the proportion of the population living under the conditions $Z < Z_*$ and $p_{\text{density}} > p_*$ was equal to 50%. The result of the calculations of the average values and parameters is given in Table 4.

Table 4. A set of average heights and suitable parameter values

$\bar{Z}$	$\bar{Z}_{\text{population}}$	$\bar{Z}_{\text{population},50\%}$	Z_*	p_*
804,9 m	442,9 m	61,3 m	187,5 m	2 people/sq.km

According to Table 4, the average height of land is 804,9 meters. Weighted average height of the land, taking into account the population density, roughly speaking, is half the size, more precisely, 442,9 m. Finally, 50% of the population lives within the height of 187,5 m, while the average weighted height of the settlement, taking into account the density of the population, is 61,3 m. The last mean value characterizes the well-known fact that half of the population is concentrated in the vicinity of the coastline of the world ocean.

Figure 7 shows two maps of settlement of 50% of the population concentrated near the coastal edge and provided that the density of the population exceeds the selected threshold p_*. Figure 7,a shows the coastline (red) and region of settlement population (toned in blue). On the map Figure 7,b with different colors in a separate closed polygons that meet the conditions that people live at altitudes not exceeding the value of Z_* with a density of population exceeding the value of p_* are shown. In this calculation, the total number of such

[2] The relief data was taken from the Mapping Toolbox of the MATLAB package.

polygons was 932, while the shoreline is not marked, but it is readily apparent in the position of the polygons.

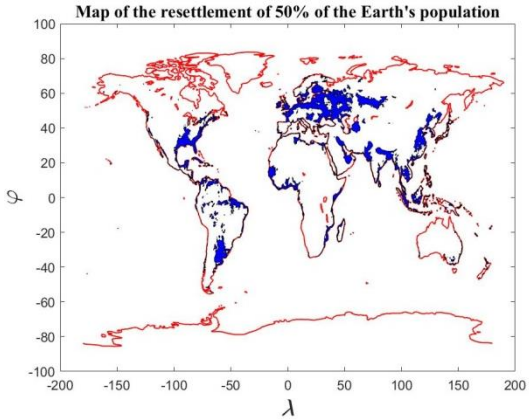

Figure 7,a. Map of the resettlement of 50% of the Earth's population (overall perspective)

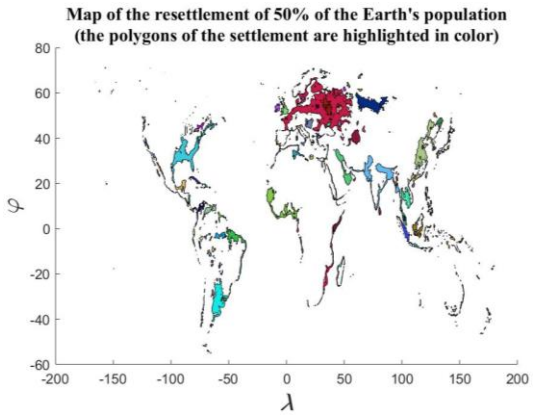

Figure 7,a. Map of the resettlement of 50% of the Earth's population (multi-polygonal perspective)

The above considerations on the relationship between the relief and the population density of the Earth's population speak of their complex interrelationship. In particular, it is not possible to introduce a comfortable value of the altitude, like comfortable temperature and precipitation.

We will solve the problem of identifying areas on which 50% of the total capacity of the habitat U is concentrated. These territories can be found from the condition that the heights do not exceed a certain threshold value Z_ρ, and the density of the medium capacity exceeds a certain threshold value p_ρ. As the density of the capacity of the habitat, we take function (3) with parameters from point #5 of Table 1. We define the weighted average height $\bar{Z}_{\text{capacity}}$, where the density of the medium capacity ρ, appears as the weight, and also the average weighted average over the territories, $\bar{Z}_{\text{capacity},50\%}$, where 50% of the total capacity of the medium is concentrated. Similarly to (14) we write the formula for calculating the weighted average height:

$$\bar{Z}_{\text{capacity}} = \frac{\sum_{i,j} Z_{i,j}\rho_{i,j}\cos\varphi_i}{\sum_{i,j}\rho_{i,j}\cos\varphi_i}, \qquad (15)$$

where the summation in (15) propagates over those pairs (i,j), for which $Z_{i,j} > 0$.

Table 5. A set of weighted average heights and suitable thresholds for parameters taking into account the density of the medium's capacity

$\bar{Z}_{\text{capacity}}$	$\bar{Z}_{\text{capacity},50}$	Z_ρ	p_ρ	U
714,5 m	312,1 m	820 m	1,82	7,7039

Table 5 shows a set of parameter values, which is the solution for the problem formulated above.

The parameters given in Table 5 allow us to find the areas where 50% of the habitat capacity is concentrated. These are the territories that are within the height $Z_\rho = 820$ m, and the values of the density of the habitat capacity exceed the value $p_\rho = 1{,}82$. In Figure 8 maps are constructed that illustrate the positioning of the 741 territories that fall within these limits. On the left map of Figure 8 the search area is shaded one color and on the right the map different colors.

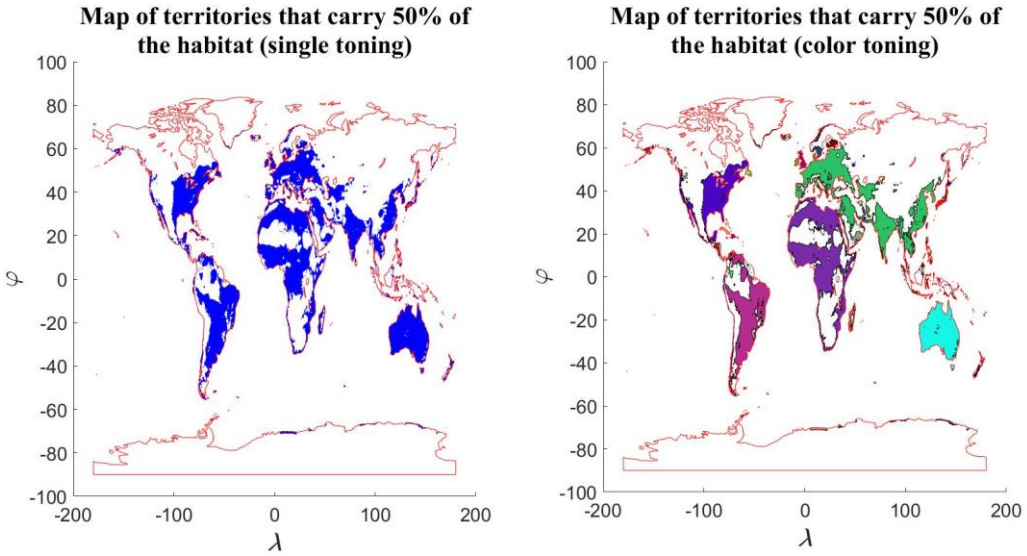

Figure 8. Map of territories that carry 50% of the habitat capacity in different tints: a single toning (left map) and tinting of territories with different colors (right map)

Note that the maps in Figure 7 and Figure 8 differ rather significantly. This can be explained as follows. The density of the Earth's population, which was used as the weight in formulas (14), varied in the range $[1{,}04;10^4]$. The density of the capacity of the habitat, which was used as the weight in formula (15), varied in the range [0,77;15,26]. A couple of bands differ from each other in 690 times. In other words, the population of the Earth due to high density, i.e. by concentrating in large urban agglomerations, "economize" on space. Furthermore were calculated square accommodations 50% of the population, $S_{\text{population}}$ and square seats concentration 50% capacity, S_{capacity}, represented in Figure 7 and 8. It turned out that $S_{\text{population}} = 0{,}5131 \cdot R^2$, $S_{\text{capacity}} = 2{,}1120 \cdot R^2$, where R is the radius of the Earth's. Thus, the surface of living 50% of the population in 4 times less the surface of the positioning 50% of the habitat capacity.

Maps in Figure 8 can be viewed from a different perspective by constructing a density gradient field of the habitat capacity. We define in the spherical coordinate system a two-component gradient vector $\boldsymbol{g} = \nabla\rho$ of the density of the habitat capacity in the form:

$$\boldsymbol{g} = \left(\frac{\partial\rho}{\partial\varphi}, \frac{1}{\cos\varphi}\frac{\partial\rho}{\partial\lambda}\right). \qquad (16)$$

The density of the habitat capacity is considered on a grid with a resolution of half a degree.

To approximate the derivatives in (16), we take the four-point pattern, then we write

$$\left(\frac{\partial\rho}{\partial\varphi}\right)_{i,j} = \frac{60}{\pi}(\rho_{i+1,j}+\rho_{i+2,j}-\rho_{i-1,j}-\rho_{i-2,j}), \quad (17)$$

where $i = 3, \dots, 357$; $j = 1, \dots, 720$ and

$$\left(\frac{1}{\cos\varphi}\frac{\partial\rho}{\partial\lambda}\right)_{i,j} = \frac{60}{\pi\cos\varphi_i}(\rho_{i,j+1}+\rho_{i,j+2}-\rho_{i,j-1}-\rho_{i,j-2}), \quad (18)$$

where $i = 1, \dots, 360$; $j = 1, \dots, 720$, it is assumed that in (18) a periodic extension with respect to the index *j* with period 720.

Figure 9 shows the gradient field as a set of arrows, $\boldsymbol{g_{i,j}} = (\frac{\partial\rho}{\partial\varphi}, \frac{1}{\cos\varphi}\frac{\partial\rho}{\partial\lambda})_{i,j}$ of the density of the medium, calculated by formulas (16) — (18) with density of the habitat capacity (3) with parameters from point #5 of Table 1.

In Figure 9, clearly in the form of a "fringe" of arrows, a noticeable increase the density of the capacity habitat is seen as it approaches to the shoreline, which once again confirms the well-known fact that half of the world's population lives in the vicinity of the coast of the world ocean.

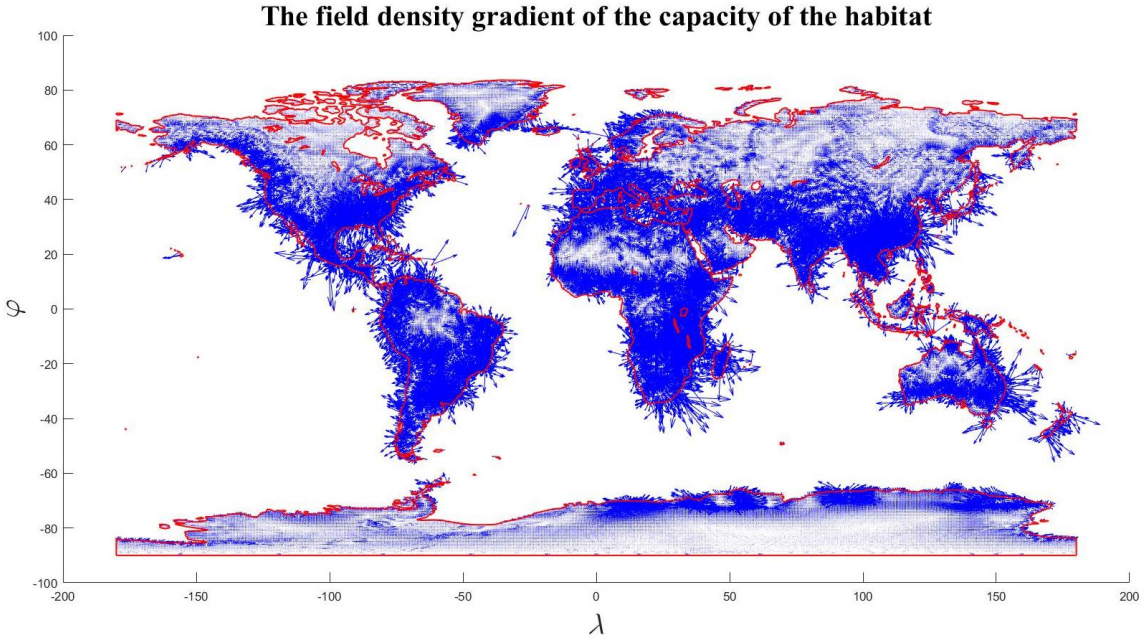

Figure 9. The field density gradient of the capacity of the habitat

SECTION IV.
CUTTING TERRITORIES IN TERMS OF "(not)HIGH – (not)FAVORABLY"

The studies presented in the previous section allow the classification, cutting of territories in terms of "high – low", "favorable – unfavorable". The term "high-low" means literally the following: the locality of residence is at an altitude higher than a certain threshold value Z_ρ or, accordingly, less. The term "favorably – unfavorable" means that the density of the habitat capacity exceeds a certain threshold value p_ρ or, respectively, less.

According to the previous section, the threshold values Z_ρ and p_ρ were found from the fact that the capacity of the habitat of the territories covered by these conditions was 50%. According to Table 5, $Z_\rho = 820$ m and $p_\rho = 1{,}82$.

Consider now the conditional space with the coordinates ρ $(0 \le \rho \le \rho_{\max})$ and Z $(0 \le Z \le Z_{\max})$ and draw two lines $\rho = p_\rho$ and $Z = Z_\rho$, then any area of habitat on the Earth can be assigned to one of the four areas on plane with coordinates ρ and Z. Under coordinate ρ we understand the density capacity of the habitat, and a coordinate Z — height of the location above sea level. Figure 10 shows the positioning of each of the four areas with an approximate preservation of the scales by coordinates.

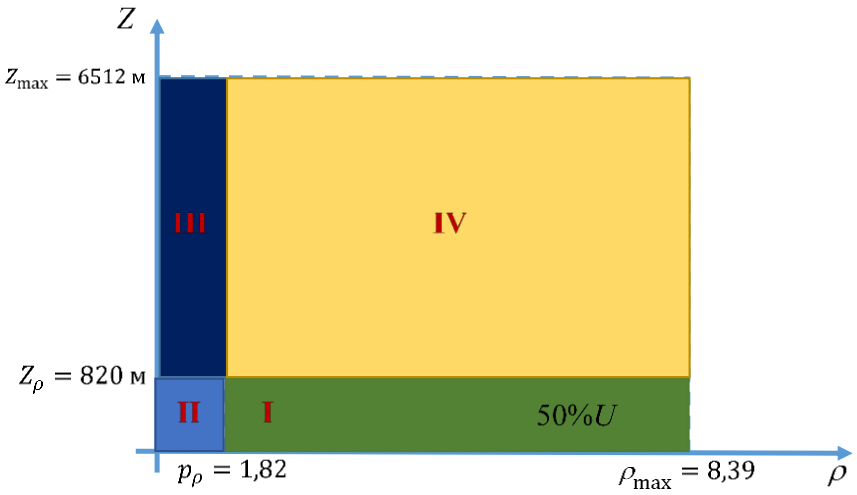

Figure 10. Positioning of each of the four areas in the space with coordinates ρ, Z

According to Figure 10, the area I is determined by a pair of conditions: $\rho > p_\rho$ and $Z < Z_\rho$; area II — $\rho < p_\rho$ and $Z < Z_\rho$; area III — $\rho < p_\rho$ and $Z > Z_\rho$; area IV — $\rho > p_\rho$ and $Z > Z_\rho$. In terms of "highly favorable": the first area is most conducive to living, i.e. these territories are not very high, and they are climate-friendly; the second area corresponds to areas that are not very high, but they are unfavorable from a climatic point of view; the third area corresponds to the most severe territories, located high and which are unfavorable from the climate point of view, finally, the territories of the fourth territories, although they are located high, are favorable from the climate point of view. Figure 10 also shows the coloration specific for each type of territories used in constructing the map in Fig.12.

Figure 11 shows four maps of the territories corresponding to each of the four squares in Figure 10. Territories within a separate category are colored in Figure 11 by random colors. The initial data were taken according to calculations of the previous section. The results of calculations of the areas of territories, volumes of capacities of the environment and the number of territories for each of the types are given in Table 6.

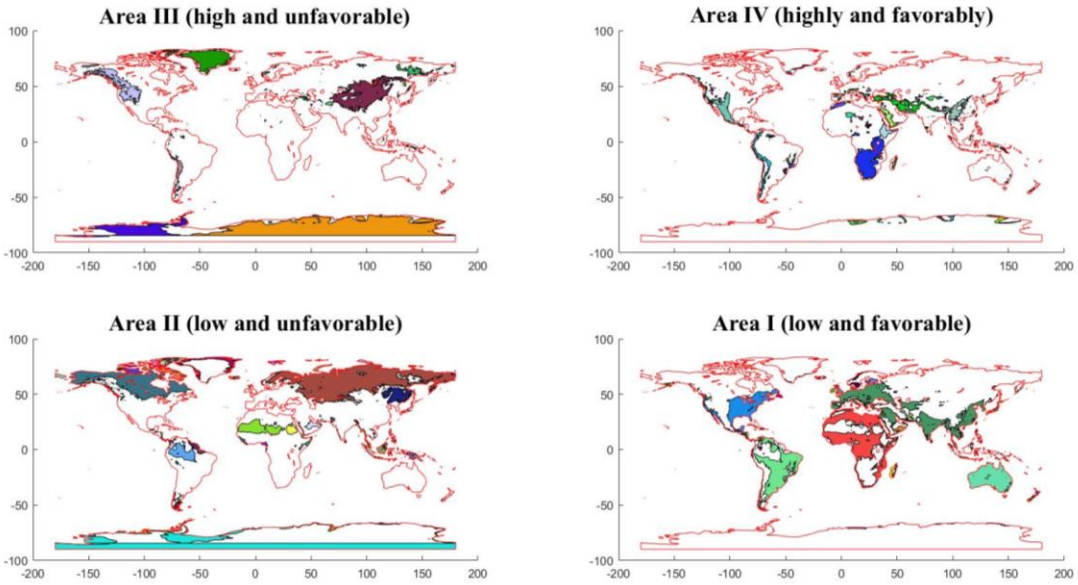

Figure 11. Maps of the territory with parameters of density of capacity of habitat and height of positioning according to four areas

The squares of areas in the Table 6 are given in units of R^2, where R is the radius of the Earth. In particular, if the whole territory of the first territory is selected as the unit, the ratio of the areas of all four types of territories will be 1: 0,59: 0,35: 0,30. Finally, if the total capacity of the habitat of the territories of the first area is chosen as the unit, the ratio of the capacities of the habitat of all four types will be 1: 0,41: 0,21: 0,38.

Table 6. A set of areas (S), volumes of habitats (U) and the number of territories (N) for each of the areas

Variable	Area I	Area II	Area III	Area IV	Sum
S/R^2	1,7909	1,0632	0,6276	0,5420	4,0237
U	3,8525	1,5796	0,8095	1,4623	7,7039
N	391	473	401	454	1719

In Figure 12,a shows a single map for the territories of all four qualities, while the site of the first area are colored green, the second area is blue, the third area in violet and finally the fourth is yellow.

Let us consider in more detail the map depicting the state border of the Russian Federation (for 2008), as well as the territories classified according to Figure 10. The result is shown

in Figure 12,b. It is clearly seen from Figure 12,b that practically the entire territory of the Russian Federation is painted in blue, it is classified as “low – unfavorable”. A small fragment of the territories of the first category “low – favorably” (painted in green) is located in the west of the country.

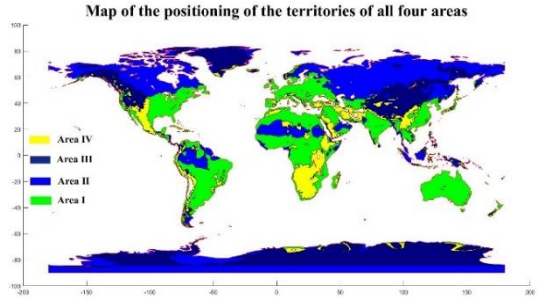

Figure 12,a. Map of joint positioning of territories of all four areas

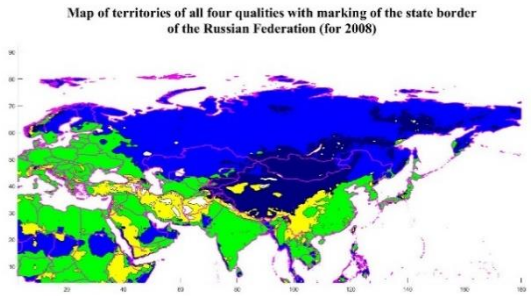

Figure 12,b. Map of territories of all four qualities with marking of the state border of the Russian Federation (for 2008)

We will calculate the so-called “index of the diversity of territories”, D for all countries and territories, the list of which was considered earlier in section III. To do this, we define the concept of “territory index”, h, which can take values from the set (1; 0,41; 0,21; 0,38), introduced above in connection with the mutual subordination of the habitats of four types of territories. Define the index of the territory for each of the points of the grid 360×720, then we obtain the matrix $h_{i,j}$, $i = 1, \dots, 360$; $j = 1, \dots, 720$. In Section III, the database for 2008 was reviewed for 246 states and territories for which we will find the indices of the diversity of territories D_k, $k = 1, \dots, 246$.

The index of diversity in an arbitrary territory is defined as the variance of the values of the territory index, i.e.

$$D_k = \text{var}\{h_{i,j}, (\varphi_i, \lambda_j) \in \omega_k,\ i = 1, \dots 360, j = 1, \dots, 720\}, \quad (19)$$

where var — variance operation, ω_k — area occupied by the k-th state or territory on the Earth sphere, $k = 1, \dots, 246$.

The territory diversity index (19) was calculated for all 246 States and territories. Figure 13 shows a fragment of the summary data for the selected set of States. If, for example, to compare the indices of the diversity of the territories of the USA and of the Russian Federation, this ratio will be equal to $D_{\text{USA}}/D_{\text{RF}} = 4{,}894$. Thus, the territory of the Russian Federation is about five times less diversity then the territory of United States. This means that the management of the US territory as an integrity is more complex than the similar management of the territory of the Russian Federation.

As a result of the studies presented in this and the previous sections, the following was revealed. Most of the population of the Earth seeks to live in territories classified as “not highly – favorable” or, in other words, closer to the land-ocean interface. This half of the

population is the most socially mobile, because it is oriented to the ocean, more precisely, to ocean traffic. Another, more conservative part of the population, is oriented to land and, consequently, continental traffic. These considerations reproduce the opposition of two political doctrines conventionally called “thalassocracy” and “tellurocracy”, well known in geopolitics (H.J. Mackinder [7], K. Haushofer [8] and several other authors), the first of which is oriented toward acquiring political power through the ocean, and the second — through the continent.

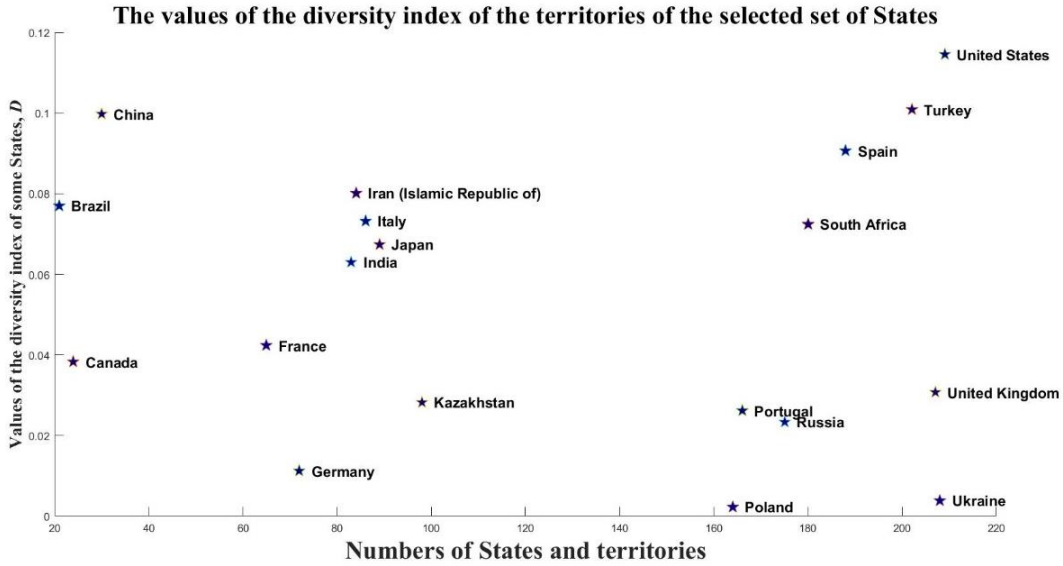

Figure 13. The values of the diversity index of the territories of the selected set of States

In this section, the cutting of land territories in terms of “(not)high — (not)favorable” is presented (Figure 12). This cutting can be considered as a prerequisite or a framework for explaining the existing configuration of State boundaries. It is clear that in the final explanation of the configuration of States borders there is always a fair share of the prehistory of the formation of a State (territory) in a single context of the world political system. In this section, we were also interested in the unification and classification of territories in terms of climatic data and relief.

Consider in the future a different method of cutting of territories, in which the decisive role is played by traffic. This way of regionalization should take into account both geopolitical features (thalassocracy and tellurocracy) of territories management.

In the beginning, we will develop an algorithm for the random distribution of a set of points on the land surface, taking into account the density of the habitat capacity. In the future, we will determine the traffic between points, the cost of traffic and, accordingly, determine the task of minimizing the cost of traffic by optimally moving the points serving as logistic nodes between the territories. The optimal position of the set of communication nodes and the coastline will determine the desired territorial subunits — geopatoms.

SECTION V.
RANDOM DISTRIBUTION OF POINTS ON THE EARTH'S SURFACE

We represent the integral in (8) as a sum in the following way. Define within the environment on the surface of the Earth N points with the coordinates $z_i = (\varphi_i, \lambda_i)$, $i = 1, \dots, N$. We will assume that all points are localized within the land. Let each point z_i corresponds to some region ω_i. As a result of the above considerations, the global capacity of the habitat (8) can be rewritten as:

$$U = \sum_{i=1}^{N} u_i \,, u_i = \iint_{\omega_i} d\varphi d\lambda \cos\varphi \cdot \rho. \qquad (20)$$

Using the Monte Carlo method, we will play the procedure of random application of N points within the land. It is necessary to play a two-dimensional random variable $z = (\varphi, \lambda)$, containing the components of latitude and longitude. Taking into account the previous sections, consider a grid of latitude and longitude values with a resolution of $0{,}5^0$. In this case, the two-dimensional random variable z will take the set of values $z_{i,j} = (\varphi_i, \lambda_j)$, $i = 1, \dots, 360$; $j = 1, \dots, 720$. We write the distribution matrix $p_{i,j}$ of the random variable z in the form:

$$p_{i,j} = p\left(z = z_{i,j}\right) = \frac{\rho_{i,j} \cos\varphi_i}{\sum_{k=1}^{360} \sum_{l=1}^{720} \rho_{k,l} \cos\varphi_k}, \qquad (21)$$

where $i = 1, \dots, 360$; $j = 1, \dots, 720$.

If we sum the matrix (21) by rows and columns, we find the series of latitude distribution, $p_{\varphi,i}$ and longitude, $p_{\lambda,j}$, i.e.

$$p_{\varphi,i} = \sum_{j=1}^{720} p_{i,j} \,, i = 1, \dots, 360; \; p_{\lambda,j} = \sum_{i=1}^{360} p_{i,j} \,, j = 1, \dots, 720. \qquad (22)$$

We construct series of distributions (22). To do this, we substitute in (21) the density of the capacity of the habitat according to formula (3) with the parameters from point #5 of Table 1. The result is shown in Figure 14.

The study of the left-hand graph in Figure 14 confirms the expectation that the probability to the poles should decrease with the random play of the latitude component of the random vector z. Taking into account the form of the density of the medium (3), it is clear that the components of the random vector z are not independent. For this reason, in order to play each of the components, it is necessary to know one of the two conditional probability matrices of the form:

$$p_{\varphi|\lambda,i,j} = \frac{p_{i,j}}{p_{\lambda,j}}, p_{\lambda|\varphi,j,i} = \frac{p_{i,j}}{p_{\varphi,i}}, \quad (23)$$

where $i = 1, \dots, 360$; $j = 1, \dots, 720$.

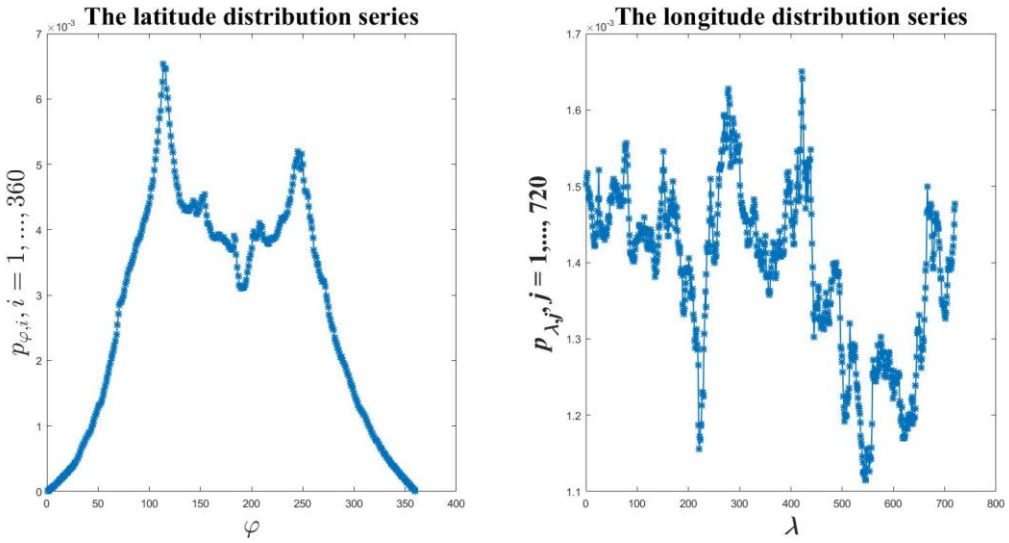

Figure 14. The series of distribution of latitude components (left graph) and longitude (right graph) of the random two-dimensional vector z

Consider the procedure for determining each of the components of the vector $z = (\varphi, \lambda)$ individually. Taking into account (22), the random variables φ and λ assume the values φ_i and λ_j with probabilities $p_{\varphi,i}$ and $p_{\lambda,j}$, where $i = 1, \ldots, 360$; $j = 1, \ldots, 720$. Prepare sets of cumulative probabilities of the following forms:

$$p_{\Sigma\varphi,i} = \sum_{k=1}^{i} p_{\varphi,k}, i = 1, \ldots, 360;\ p_{\Sigma\lambda,j} = \sum_{k=1}^{j} p_{\lambda,k}, j = 1, \ldots, 720. \qquad (24)$$

Taking into account (24), determination of the value of any of two random discrete quantities φ, λ reduces to the following procedure. For definiteness, we choose the latitude, for longitude the procedure is similar. We generate a random number ξ uniformly distributed on the interval [0;1]; find the number of the interval from the set $[0; p_{\Sigma\varphi,1}]$, $[p_{\Sigma\varphi,1}; p_{\Sigma\varphi,2}]$, …, $[p_{\Sigma\varphi,359}; p_{\Sigma\varphi,360}]$, in which a random number ξ falls. Denote the resulting number by the expression $i(\xi)$, then the played value of the random variable φ will be $\varphi_{i(\xi)}$.

Let's go back to determination of the values a two-dimensional random variable $z = (\varphi, \lambda)$. Suppose, for example, that the latitude is determined out and that the value $\varphi_{i(\xi)}$ is obtained. We need to determine the longitude at a certain latitude $\varphi_{i(\xi)}$, i.e. it is necessary to use the conditional probability $p_{\lambda|\varphi,i,j}$ from (23), when $i = i(\xi)$. In other words, the problem reduces to determining a conditional discrete random variable $\lambda|\varphi = \varphi_{i(\xi)}$, that takes the values $\lambda_1, \ldots, \lambda_{720}$ with probabilities $p_{\lambda|\varphi,1,i(\xi)}$, …, $p_{\lambda|\varphi,720,i(\xi)}$. We apply a procedure similar to the latitude determination, i.e. find the corresponding cumulative sets, generate a random number η uniformly distributed on the interval [0;1] and determine the interval number $j(\eta)$, which gets a random number η.
As a result of the above algorithm, the procedure for determining the two-dimensional random variable $z = (\varphi, \lambda)$ is completed, and generation of the pair $(\varphi_{i(\xi)}, \lambda_{j(\eta)})$ can be continued without restrictions. In specific calculations, the algorithm was somewhat

different. Let N value pairs $(\varphi_{i(\xi_n)}, \lambda_{j(\eta_n)})$, $n = 1, \dots, N$ be generated. For even values of n, the latitude was first determined, and then, using the conditional probability, longitude was determined and, conversely, for odd n, longitude was determined first, and then with the conditional probability the latitude was determined.

Figure 15 shows the result of the application described above in the form of one of the versions of the random application of $N = 10^3$ points within the land, taking into account the density of the habitat.

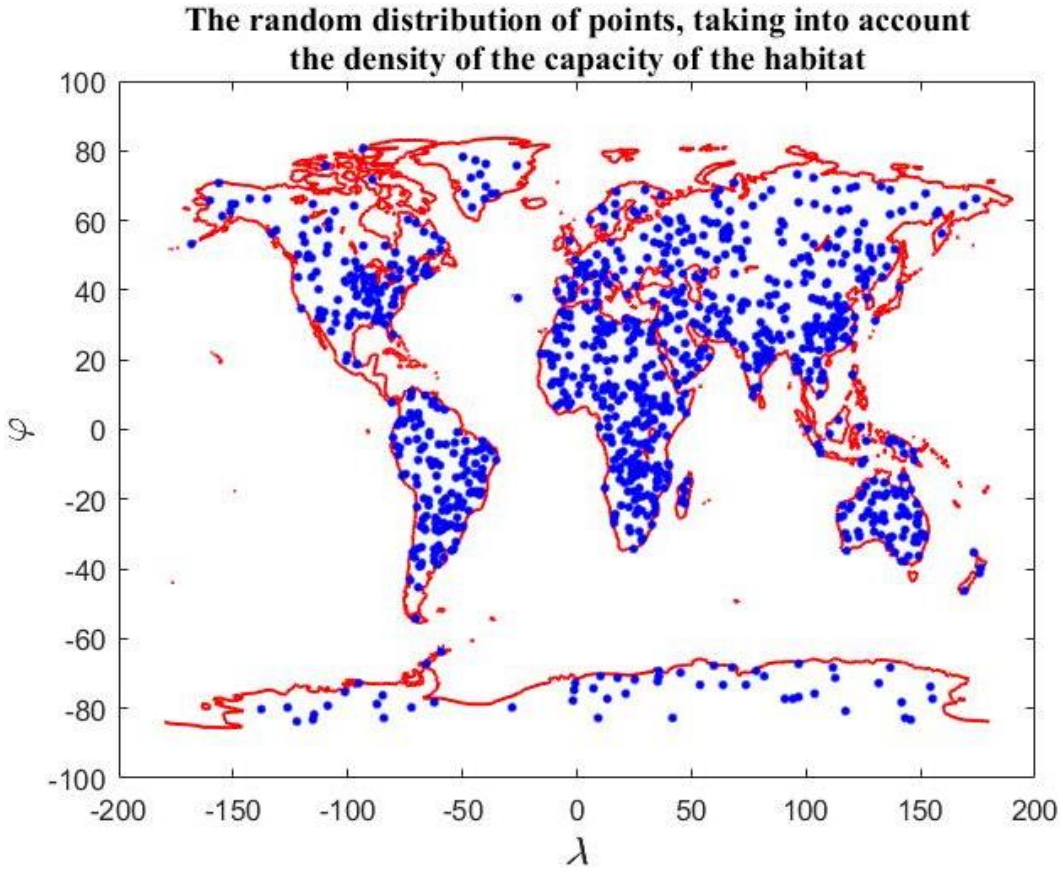

Figure 15. The random distribution of $N = 10^3$ points, taking into account the density of the capacity of the habitat

SECTION VI.
TRAFFIC BETWEEN TERRITORIES

Consider the presence of correspondence or traffic between a pair of territories with numbers i and j $(i, j = 1, \dots, N)$. In the previous section, an algorithm was developed for the random distribution of N points on the Earth's surface, taking into account the density of the capacity of the habitat. With each of the points we associate a certain territory, which will have corresponding a capacity habitat u_i, $i = 1, \dots, N$. As such territories, we take Voronoi polygons for a finite set of points $z_i = (\varphi_i, \lambda_i)$, $i = 1, \dots, N$ on the surface of the Earth. A set of N points can be interpreted, among other things, as logistics nodes for transporting part of the habitat capacity between territories.

Figure 16 shows an example of the distribution by the Monte Carlo method of $N = 10^3$ points on the Earth's surface, taking into account the procedure (21) — (24). There, along with the shoreline and poles, the corresponding Voronoi polygons are plotted. When constructing the Voronoi polygons in the latitude-longitude coordinates, a singularity associated with the poles took place. Four additional "fictitious" points were introduced: $z_{N+1} = \chi(90^0, 180^0)$, $z_{N+2} = \chi(-90^0, 180^0)$, $z_{N+3} = \chi(-90^0, -180^0)$, $z_{N+4} = \chi(90^0, -180^0)$, where $\chi = \text{const} > 0$. In the calculations, the parameter χ was chosen equal to 5. Next, Voronoi polygons were found from the extended set of points $z_i = (\varphi_i, \lambda_i)$, $i = 1, \dots, N, N+1, N+2, N+3, N+4$. In the framework of this procedure, Voronoi finite polygons are guaranteed to include the coastline, and unbounded polygons were moved to the fictitious area.

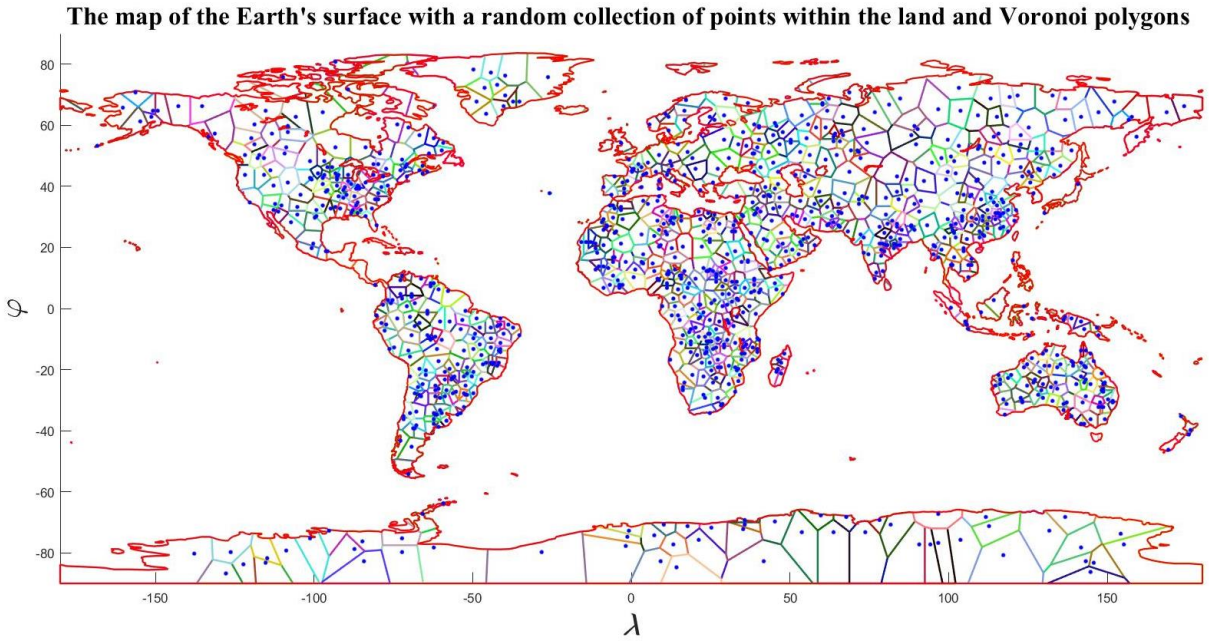

Figure 16. The map of the Earth's surface with a random collection of $N = 10^3$ points within the land and Voronoi polygons

In the beginning we will define the traffic, escort of which is cost-free. We define the matrix $\alpha_{i,j}$, $i,j = 1,\dots,N$, the elements of which characterize the transfer of the i-th fraction of the habitat capacity to the j-th fraction of the habitat capacity in connection with traffic. The matrix $\alpha_{i,j}$, $i,j = 1,\dots,N$ acts as a measure for the exchange of the capacity of the habitat between a set of points $z_i = (\varphi_i, \lambda_i)$, $i = 1,\dots,N$ on the Earth's surface. According to the definition, it follows that

$$\sum_{j=1}^{N} \alpha_{i,j} = 1, \quad (25)$$

where $\alpha_{i,i}$ — the share of the i-th capacity of the habitat is not subject to traffic, i.e. this is the fraction that remains inside the i-th territory. The set of capacities of the habitat u_i, $i = 1,\dots,N$ acts as some resource that in the context of traffic is considered universal and additive.

We find the amount of habitat capacity, $U_i^{(-)}$ left due to traffic the i-th territory and the corresponding amount of habitat capacity, $U_i^{(+)}$ arrived in the i-th territory, then

$$U_i^{(-)} = \sum_{j=1, j\neq i}^{N} \alpha_{i,j} u_i \,, U_i^{(+)} = \sum_{j=1, j\neq i}^{N} \alpha_{j,i} u_j. \qquad (26)$$

Taking into account (25), it can be established by direct verification that there is a balance of arrival and departure of the habitat capacity, $\sum_{i=1}^{N} U_i^{(-)} = \sum_{i=1}^{N} U_i^{(+)} = \sum_{i=1}^{N} (1 - \alpha_{i,i}) u_i$, i.e. due to the cost-free traffic, how much it takes so much and comes.

Now, if we move a part of the habitat from point i to point j, the share of the resource $\gamma_{i,j}$ due to traffic is lost, we assume that $0 \le \gamma_{i,j} \le 1, i \neq j;\ i,j = 1,\dots,N$. We believe that within the logistic point there are no costs, i.e. $\gamma_{i,i} = 0, i = 1,\dots,N$. The matrix $\gamma_{i,j}, i,j = 1,\dots,N$ is called the transport cost matrix. Taking into account (26) we will form the functional, Tr of all transport costs:

$$Tr = \sum_{i=1}^{N} \sum_{j=1, j\neq i}^{N} \alpha_{i,j} \gamma_{i,j} u_i + \sum_{i=1}^{N} \sum_{j=1, j\neq i}^{N} \alpha_{j,i} \gamma_{j,i} u_j. \qquad (27)$$

The meaning of the transport functional (27) is transparent: when the resource is moved from point i to point j, its part in quantity $\gamma_{i,j}$ is consumed, similarly, when the resource is moved from point j to point i, the resource part in quantity $\gamma_{j,i}$ is also expended. The transport functional (27) can be simplified somewhat, taking into account that the first and the second double sums are the same, this is seen after renaming the indices, i.e.

$$Tr = 2 \sum_{i=1}^{N} \sum_{j=1, j\neq i}^{N} \alpha_{i,j} \gamma_{i,j} u_i. \qquad (27')$$

Using the formula (27′) we can put the optimization problem of minimizing the cost of the traffic $Tr(z_1,\dots,z_N)$ by a suitable displacement of the $z_1,\dots,z_N$ points within the land. It is clear that the global minimum cost of transport is zero value, when $Tr = 0$. In a mathematical form, the minimization problem reduces to finding a set of points $\{z_1^*,\dots,z_N^*\}$, which may not be unique, in which one of the local cost minimums for traffic is realized, i.e.

$$Tr(z_1^*, \dots, z_N^*) = \min_{z_1,\dots,z_N} Tr(z_1, \dots, z_N). \qquad (28)$$

For further progress in solving of the optimization problem (28), additional clarification of the form of the matrices $\alpha_{i,j}, \gamma_{i,j}, i, j = 1, \dots, N$ is needed. Let us consider the well-known in the theory of transport flows the so-called gravitational model [9, 10], in which some generalized "distance" $d_{i,j}$ $(d_{i,j} \geq 0)$ is introduced between the i-th and j-th territories. Note that the distance matrix $d_{i,j}$, $i, j = 1, \dots, N$, in general, is not symmetric, i.e. $d_{i,j} \neq d_{j,i}$, whereas by definition it is assumed that $d_{i,i} = 0$, $i = 1, \dots, N$. Note that the condition $d_{i,j} = 0, i \neq j$ does not necessarily imply that the z_i and z_j points are the same in the physical space.

We choose the exponential dependence of the coefficients of the matrix $\alpha_{i,j}$, $i, j = 1, \dots, N$, on the distance, then we can write the following representation:

$$\alpha_{i,j} = \frac{e^{-\beta d_{i,j}}}{\sum_{k=1}^{N} e^{-\beta d_{i,k}}}, \qquad (29)$$

where β — some nonnegative parameter. One can verify by direct verification that the condition (25) holds for the matrix $\alpha_{i,j}$, $i, j = 1, \dots, N$ in the form (29).

Following the exponential dependence of the matrix $\alpha_{i,j}$, $i, j = 1, \dots, N$ on the distance in (29), we choose the following simplest representation for the transport cost matrix:

$$\gamma_{i,j} = \tfrac{1}{2} r(1 - e^{-\beta_2 d_{i,j}}), \qquad (30)$$

where r and β_2 — some constant nonnegative coefficients. According to (30), for $d_{i,j} = 0$ there is no transportation cost, i.e. $\gamma_{i,j} = 0$. Finally, for $\beta_2 \to \infty$ and for $d_{i,j} \neq 0$ it follows that $\gamma_{i,j} \to \frac{1}{2} r$, i.e. the share of transport costs becomes a constant value of $\frac{1}{2} r$. The last remark implies that $0 \leq r \leq 2$.

We substitute (29), (30) into (27′), then we find the following expression for the total transport costs:

$$Tr = r \sum_{i=1}^{N} [1 - \sum_{k=1}^{N} e^{-(\beta+\beta_2) d_{i,k}} / \sum_{k=1}^{N} e^{-\beta d_{i,k}}] u_i. \qquad (27'')$$

The transport costs in the form (27′′) are characterized by the following properties, which are checked directly. First, when the distance between the points becomes zero, i.e. $d_{i,j} = 0, i, j = 1, \dots, N$, there are no transportation costs, $Tr = 0$. Secondly, when the distance between points tends to infinity, i.e. $d_{i,j} \to \infty, i \neq j; i, j = 1, \dots, N$, the transport costs due to the selected dependencies (29), (30) also tend to zero, $Tr \to 0$. Note that a distance of zero or infinity between two points does not mean that the points merge or diverge to infinity.

Consider transport costs in the form (27′′) as a function of the parameter β_2, i.e. $Tr = Tr(\beta_2)$. In this case it is obvious that $Tr(0) \equiv 0$. Now let $\beta_2 \to \infty$, then $Tr(\beta_2) \to Tr(\infty) = r\sum_{i=1}^{N}[1 - 1/\sum_{k=1}^{N} e^{-\beta d_{i,k}}]u_i$. For the last transport cost functional, it is obvious that the global minimum equal to zero is achieved only when the distances between points tend to infinity. The latter case will be considered in the future from the point of view of computational experiment. In this case, the points cannot come together, they will repulse and fill the maximum of the habitat, because they are "locked" on the surface of the terrestrial sphere.

The condition of the transition limit $\beta_2 \to \infty$ we call "the minimax transport doctrine", which means the minimum transport costs at a maximum filling capacity of the habitat.

We substitute (27′′) in (28), then in the general case the problem of minimizing transport costs will be rewritten in the form:

$$Tr(z_1^*, \dots, z_N^*) = \min_{z_1,\dots,z_N} r\sum_{i=1}^{N}[1 - \frac{\sum_{k=1}^{N} e^{-(\beta+\beta_2)d_{i,k}}}{\sum_{k=1}^{N} e^{-\beta d_{i,k}}}]u_i. \qquad (31)$$

To clarify the problem of minimizing (31) in a simplified form, when it is assumed that $\beta_2 \to \infty$, i.e. there is a minimax transport doctrine, then

$$Tr(z_1^*, \dots, z_N^*) = \min_{z_1,\dots,z_N} r\sum_{i=1}^{N}(1 - \frac{1}{\sum_{k=1}^{N} e^{-\beta d_{i,k}}})u_i. \qquad (31')$$

In order to determine the algorithm for calculating the distance matrix $d_{i,j}$, $i, j = 1, \dots, N$ we will give a series of physical considerations on the energy costs of moving one unit of cargo weight from $z_1 = (\varphi_1, \lambda_1)$ to $z_2 = (\varphi_2, \lambda_2)$. Let the route of movement of freight is defined in the form of a line: $\varphi = \varphi(s)$, $\lambda = \lambda(s)$, $0 \le s \le l$. The argument of the line parametrization is the length of the line, s, changing from zero to its maximum value, l, equal to the length of the route, while it is assumed that $\varphi_1 = \varphi(0)$, $\lambda_1 = \lambda(0)$ and $\varphi_2 = \varphi(l)$, $\lambda_2 = \lambda(l)$.

Let in the beginning the route of movement is completely located on the surface of the land. In this case, the energy cost of moving one conventional unit of cargo weight consists of three characteristic variants of movements: 1) vertical movement of cargo upwards due to the peculiarities of the relief; 2) vertical lowering of cargo due to the peculiarities of the relief; 3) movement of cargo along an inclined surface. The first two points of the variants of the movement describe the energy costs of moving the load "up and down". The last point is mainly characterized by energy costs to overcome rolling friction within the framework of such modes of transport as road and rail. Let $Z = Z(\varphi, \lambda)$ be the relief of the land surface, then for the selected route of movement of the conventional unit of cargo mass, we can write the function $Z(s) = Z(\varphi(s), \lambda(s))$, $0 \le s \le l$.

Taking into account the stated physical considerations, we will write the formula for calculating the distance along the chosen trajectory between a pair of points z_1 and z_2, d_{earth}:

$$d_{\text{earth}} = g_1 \int_0^l \frac{dZ}{ds}\kappa\left(\frac{dZ}{ds}\right)ds - g_2 \int_0^l \frac{dZ}{ds}\kappa\left(-\frac{dZ}{ds}\right)ds + g_3 \int_0^l \sqrt{1-\left(\frac{dZ}{ds}\right)^2}ds, \quad (32)$$

where $\kappa(t) = 1$, $t \geq 0$; $\kappa(t) = 0$, $t < 0$ — so-called "single" function. The unknown non-negative parameters g_1, g_2, g_3 characterize the contribution of each of the types of movements for the displacement of one conventional unit of cargo mass. The integrals in (32) are called transport integrals.

Let now the route of movement of one conventional unit of mass of cargo lies entirely in the sea, i.e. the points of departure, arrival, and all other points of the route lie on the surface of the sea. In this case, the energy costs associated with the movement of one unit weight of the conventional cargo by sea transport are associated with the overcoming of viscous friction. To calculate the distance along the selected path between a pair of points z_1 and z_2, d_{sea} one can use formula (32). We believe that water transport moves along a horizontal surface, for which it can be assumed that $dZ/ds = 0$. Taking into account the last integral in (32) and performing elementary integration, we write the corresponding transport integral in the form:

$$d_{\text{sea}} = g_4 l, \quad (33)$$

where g_4 — a certain nonnegative parameter that takes into account the averaged features of viscous friction in the water environment of the aggregate water transport.

Note that an arbitrary route between points of departure and of destination can be broken down into stages of the movement only on land or only at sea. Applying either formula (32) or formula (33) to each step and adding the values obtained, we find the total distance between a pair of points. Distances calculated by formulas (32), (33), are not distances in the usual sense of the word. They rather act as effective distances, which can always be measured by calculating the average energy of the movement of one conventional unit of mass of cargo from the point of departure to the destination.

Based on physical considerations, we estimate the order of magnitude of the parameters g_1, g_2, g_3, g_4. When lifting a load on an inclined plane, work in the part of lifting is expressed by the formula: $mg\frac{dZ}{ds}ds$, where m — cargo mass, and g — acceleration of gravity. Let us find the specific work per unit of cargo weight by dividing by mg, it is $\frac{dZ}{ds}ds$, i.e. $g_1 = 1$.

A somewhat different situation when moving cargo along the inclined plane in the case of descent. It is not clear how much the average energy for conventional land transport (road and rail) is required for descent. The simplest case is to assume that the same amount of energy is required as in the ascent, then we find $g_2 = 1$.

To evaluate the third parameter, it is necessary to take into account the formula for determining the friction of rolling. Let f be the friction of rolling, and R is the radius of the

wheel, then we can write the following formula for working on overcoming the rolling force: $\frac{f}{R}mg\sqrt{1-(\frac{dZ}{ds})^2}ds$. Note that the friction of rolling rubber on asphalt for motor vehicles, f_{auto} and the friction of rolling steel on steel for rail transport, f_{rail} can be considered equal in order of magnitude, i.e. $f_{\text{auto}} \cong f_{\text{rail}} \cong 0{,}5$ mm. Consider that the average wheel radius total car and wagon railway transport order 0,5 m. In this case, the specific work on moving the unit of cargo weight will be $\frac{f}{R}\sqrt{1-(\frac{dZ}{ds})^2}ds$. Substituting $f = 0{,}5 \cdot 10^{-3}m$ and $R = 0{,}5m$, we find $g_3 \cong 10^{-3}$.

We now proceed to estimate the numerical coefficient g_4. To do this, calculate the force of resistance R for a typical container ship [11] with dimensions: length, $L = 157$m; width, $B = 25{,}4$m; draught, $T = 9{,}22$m, displacement, $D = 22800$ ton; design speed, $v = 19$ knots $= 9{,}77$m/s. To calculate the resistance force of friction it is common to use the formula $R = \xi\frac{\rho v^2}{2}\Omega$, where ξ is the complex aggregate friction coefficient, ρ is the seawater density, Ω is a wetted surface of ship's hull. We divide the force of resistance by the weight of the vessel, equal to $mg = \rho_* Vg$, ρ_* is an average mass density of a ship with a cargo, V is the volume of the ship, approximately its displacement, g means the acceleration of gravity. As a result, we can write the following estimate for the sought coefficient: $g_4 = \xi\frac{\rho\, v^2\Omega}{\rho_* 2gV}$. We believe that $\xi \cong 10^{-3}$, $\rho \sim \rho_*$. The value of the wetted surface is calculated by the formula of Muragin $\Omega = LT\left(1{,}36 + 1{,}13 \times 0{,}62 \times \frac{B}{T}\right) \cong 4{,}76 \cdot 10^3\text{m}^2$. As a result, we find $g_4 \cong 10^{-3}$. We note that within the framework of our analysis, in order of magnitude, the specific energy costs for the movement of a unit of cargo mass with the help of land and water transports are the same.

In the optimization problem (31′) a set of capacities of the environment of individual regions $u_i, i = 1, \dots, N$ were considered as fixed. However, this does not correspond to the procedure of cutting areas using Voronoi polygons. Indeed, with the optimization of the location of the points $z_1, \dots, z_N$, their positions will change, which will lead to a change in the arrangement of the corresponding Voronoi polygons. For this reason, in (31′) it is necessary to keep in mind the set of u_i, $i = 1, \dots, N$, obtained in connection with the current set of points $z_1, \dots, z_N$ and the fact that $\sum_{i=1}^N u_i = U$, where U is the capacity of the habitat within the land, u_i is the capacity of the habitat of the Voronoi polygon ω_i. As a result, the optimization problem (31′) should be rewritten as:

$$Tr(z_1^*, \dots, z_N^*) = \min_{z_1,\dots,z_N} r\sum_{i=1}^N (1 - \frac{1}{\sum_{k=1}^N e^{-\beta d_{i,k}}})u_i, \quad (34)$$

$$U = \sum_{i=1}^N u_i\,, u_i = \iint_{\omega_i} d\varphi d\lambda \cos\varphi \cdot \rho. \quad (35)$$

To solve the optimization problem (34), (35), we will use the simple iteration method, choosing the set u_i, $i = 1, \dots, N$ in (34) from the previous iteration. The search for a minimum in (34) allows us to find the set of points $z_1, \dots, z_N$ at the next iteration, by which we define a new set u_i, $i = 1, \dots, N$ and so on. Let τ be the iteration number, $\tau = 1{,}2, \dots$, then problem (34), (35) can be rewritten as:

$$Tr(z_1^{(\tau)}, \dots, z_N^{(\tau)}) = \min_{z_1,\dots,z_N} r \sum_{i=1}^{N} (1 - \frac{1}{\sum_{k=1}^{N} e^{-\beta d_{i,k}^{(\tau)}}}) u_i^{(\tau-1)}, \quad (34')$$

$$U = \sum_{i=1}^{N} u_i^{(\tau-1)}, u_i^{(\tau-1)} = \iint_{\omega_i^{(\tau-1)}} d\varphi d\lambda \cos\varphi \cdot \rho. \quad (35')$$

The optimization problem (34′), (35′) is solved iteratively until the sequences $z_i^{(0)}, z_i^{(1)}, \dots, z_i^{(\tau)}, \dots$ converge for each $i = 1, \dots, N$. It is assumed that the set $z_1^{(0)}, \dots, z_N^{(0)}$ determines the initial location of the points, and the collection $u_i^{(0)}$, $i = 1, \dots, N$ is the corresponding list of capacities of the Voronoi polygon environment.

SECTION VII.
THE METHOD OF CALCULATING OF THE DISTANCE MATRIX

To calculate the generalized distance (32), (33) between an arbitrary pair of points on the surface of the Earth $z_1 = (\varphi_1, \lambda_1)$, $z_2 = (\varphi_2, \lambda_2)$ we construct in the beginning the trajectory of a small fragment of the total circle of the Earth passing through a given pair of points. We assume that the total circle lies in the plane passing through the center of the Earth. In other words, we construct a line: $\varphi = \varphi(s), \lambda = \lambda(s)$, where s is a parameter describing the length of the fragment of the circle. We assume that $0 \le s \le \theta$, $\varphi(0) = \varphi_1, \lambda(0) = \lambda_1$ and $\varphi(\theta) = \varphi_2, \lambda(\theta) = \lambda_2$, where θ is the arc length of the fragment of the total circle of the Earth.

We define two unit vectors of length $\boldsymbol{n}_1, \boldsymbol{n}_2$, which point to a pair of selected points $z_1 = (\varphi_1, \lambda_1)$, $z_2 = (\varphi_2, \lambda_2)$, then

$$\boldsymbol{n}_k = (\cos\lambda_k \cos\varphi_k\,, \sin\lambda_k \cos\varphi_k\,, \sin\varphi_k), k = 1{,}2. \qquad (36)$$

Let the vector $\boldsymbol{n} = (n_x, n_y, n_z)$ of unit length indicate an arbitrary point of the complete circle passing through the selected pair of points. It is clear that the vector $\boldsymbol{n}$ lies in the plane formed by the vectors $\boldsymbol{n}_1, \boldsymbol{n}_2$. Taking into account (36), after simple transformations, we find

$$\boldsymbol{n} = \boldsymbol{n}(s) = \tfrac{\sin(\theta - s)}{\sin\theta}\boldsymbol{n}_1 + \tfrac{\sin s}{\sin\theta}\boldsymbol{n}_2, \qquad (37)$$

where θ is the angle between a pair of vectors $\boldsymbol{n}_1, \boldsymbol{n}_2$. According to (37), it is obvious that $\boldsymbol{n}(0) = \boldsymbol{n}_1$ and $\boldsymbol{n}(\theta) = \boldsymbol{n}_2$.

Taking into account (37), and also considering that $n(s) = (\cos\lambda(s)\cos\varphi(s)\,, \sin\lambda(s)\cos\varphi(s)\,, \sin\varphi(s))$, we find the parametric recording of the complete circle in the coordinates "latitude – longitude":

$$\varphi = \varphi(s) = \arcsin(n_z) = \arcsin[\tfrac{\sin(\theta - s)}{\sin\theta}\sin\varphi_1 + \tfrac{\sin s}{\sin\theta}\sin\varphi_2], \qquad (38)$$

$$\lambda = \lambda(s) = \operatorname{arctg}\tfrac{n_y}{n_x} = \operatorname{arctg}\frac{\sin(\theta - s)\sin\lambda_1\cos\varphi_1 + \sin s\sin\lambda_2\cos\varphi_2}{\sin(\theta - s)\cos\lambda_1\cos\varphi_1 + \sin s\cos\lambda_2\cos\varphi_2}. \qquad (38')$$

Note that the formula (38′) is true when $n_x > 0$. In the other two cases: 1) $n_x < 0, n_y > 0$; 2) $n_x < 0, n_y < 0$ to the expression in (38′) it is necessary to add and subtract π, respectively.

When carrying out a line between a pair of points, according to formulas (38), (38′), it is also necessary to find its intersection with the coast line to identify those parts of the trajectory that lie separately on land and at sea. To depict the trajectories (38), (38′), two cases must be distinguished: 1) $|\lambda_1 - \lambda_2| < \pi$; 2) $|\lambda_1 - \lambda_2| > \pi$. In the first case, the zero meridian will be placed in the center of the map, i.e. the Atlantic Ocean will be located in the

center. In the second case, after shifting the longitude $\lambda \to \lambda + \pi$, we construct a map with the center along the line of the date change, i.e., with the center in the Pacific Ocean.

Figure 17 shows an example of the positioning of ten points on the land surface. The points are chosen randomly according to the algorithm of section V, i.e. taking into account the density of the capacity of the habitat. The points are numbered and are shown in each of the two cards. In Figure 17, taking into account the spherical geometry, all $10{\times}9/2 = 45$ lines are constructed, connecting each pair of points. In addition, the lines are marked in part of their passage overland (solid line), and by sea (dashed line). According to Figure 17, some of the binary lines are positioned on the right map with the center in the Pacific Ocean.

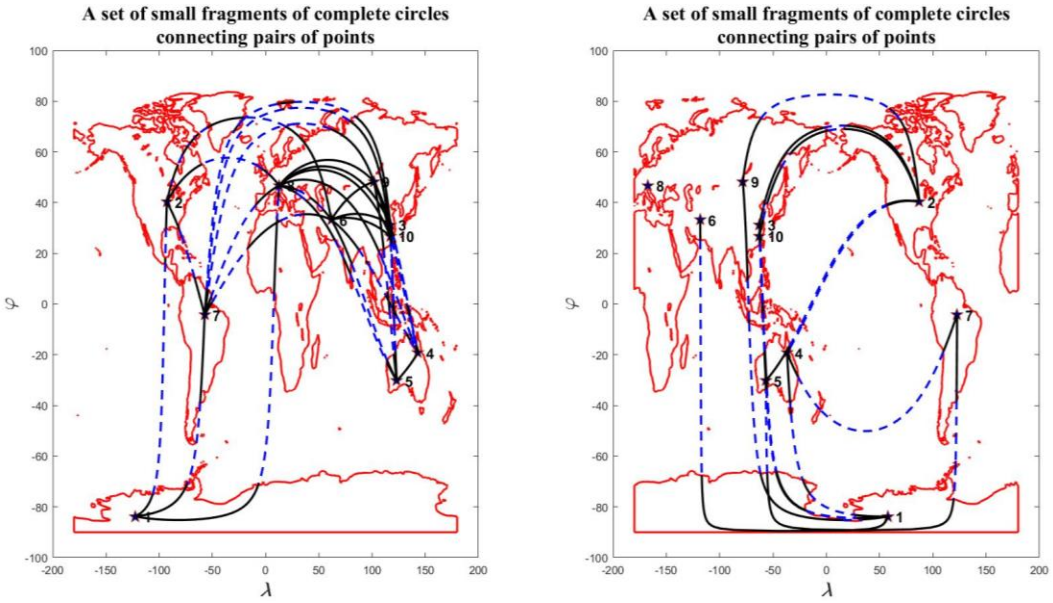

Figure 17. A set of small fragments of complete circles connecting pairs of points

According to formula (32), to calculate the effective distance on the displacement of one conventional unit of the cargo mass on the Earth's surface, it is important to know the derivative of the relief $Z = Z(\varphi, \lambda)$ along the route, which we describe with some trajectory. Let, for example, a path be established between a pair of points $z_1 = (\varphi_1, \lambda_1)$, $z_2 = (\varphi_2, \lambda_2)$ such that $\varphi = \varphi(s), \lambda = \lambda(s)$, where s is a parameter describing the distance traveled from the starting point. In this case it is obvious that $\frac{dZ}{ds} = \frac{\partial Z}{\partial \varphi}\frac{d\varphi}{ds} + \frac{\partial Z}{\partial \lambda}\frac{d\lambda}{ds}$.

As a route between a pair of points on the surface of the Earth's sphere, we choose a smaller fragment of the total circle passing through a pair of points. A suitable trajectory is presented in the form of formulas (38), (38′). It remains to find the derivatives. After simple calculations, we get:

$$\frac{d\varphi}{ds} = \frac{-\cos(\theta - s)\sin\varphi_1 + \cos s \sin\varphi_2}{\sqrt{\sin^2\theta - [\sin(\theta - s)\sin\varphi_1 + \sin s \sin\varphi_2]^2}}, \qquad (39)$$

$$\frac{d\lambda}{ds} = \frac{\sin\theta \sin(\lambda_2 - \lambda_1)\cos\varphi_1 \cos\varphi_2}{\sin^2\theta - [\sin(\theta - s)\sin\varphi_1 + \sin s \sin\varphi_2]^2}. \qquad (39')$$

Let us describe a large fragment of a complete circle passing through some pair of points on the Earth's surface. Taking into account the description of the small fragment of the complete circle (37), (38), (38′), it is expedient to parameterize the large fragment in two steps: 1) for values of the arc length parameter s from the range $[\mu, 0]$, where $\mu < 0$; 2) for the values of the arc length parameter s from the range $[\theta, 2\pi + \mu]$. We find the angle μ from the condition that the longitude (38′) coincides with the meridian of the date change, i.e. $\lambda(\mu) = -\pi$. From the solution of the last equation, we find $\mu = \mu_0$, when $\mu_0 < 0$ and $\mu = \mu_0 - \pi$, when $\mu_0 > 0$, in this case

$$\mu_0 = \arcsin \frac{\sin\theta \sin\lambda_1 \cos\varphi_1}{\sqrt{\sin^2\lambda_1\cos^2\varphi_1 - 2\cos\theta \sin\lambda_1 \sin\lambda_2 \cos\varphi_1 \cos\varphi_2 + \sin^2\lambda_2\cos^2\varphi_2}}.$$

Figure 18 shows an example of a complete circle passing through a pair of randomly selected points on the Earth's surface. The circle is divided into three arcs: 1) a small fragment of the full circle is marked with markers in the form of stars; 2) a large fragment of the total circle parametrized by a segment of the arc s from the range $[\mu, 0]$, where $\mu < 0$, is marked with pentagrams; 3) a large fragment of the complete circle, parametrized by a segment of the arc s from the range $[\theta, 2\pi + \mu]$ and is marked with hexagrams. Each of the arcs is marked with an appropriate angle. The arrow that separates the pentagrams and hexagrams indicates the date change line. After combining the second and third fragments of the arcs, we obtain a large fragment of the complete circle.

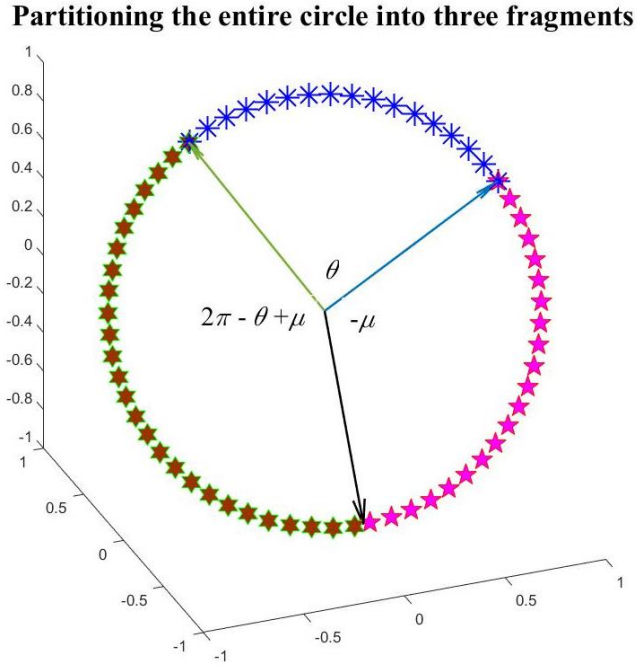

Figure 18. Partitioning the entire circle into three fragments

We introduce the distance matrix $D = \{d_{i,j}, i, j = 1, \dots, N\}$ between all pairs of points. Define similar distance matrices found for small $D_{\text{small}} = \{d_{\text{small},i,j}, i, j = 1, \dots, N\}$ and large

$D_{\text{large}} = \{d_{\text{large},i,j}, i,j = 1,\dots,N\}$ fragments of arcs of corresponding complete circles. Considering the solution of the problem of minimizing the cost of traffic, assume that the required distance matrix D is the element-wise minimum of the pair of distance matrices D_{small} and D_{large}, i.e.

$$D = \min(D_{\text{small}}, D_{\text{large}}) = \{d_{i,j} = \min(d_{\text{small},i,j}, d_{\text{large},i,j}), i,j = 1,\dots,N\}.$$

We perform a computational experiment to estimate the mean value of transport integrals in formulas (32), (33). To calculate the transport integrals, we need the partial derivatives $\frac{\partial Z}{\partial \varphi}$ and $\frac{\partial Z}{\partial \lambda}$, which we compute using the finite differences in the form (17), (18) with the resolution of the relief $0{,}5^0$; as well as ordinary derivatives $\frac{d\varphi}{ds}$ and $\frac{d\lambda}{ds}$, which we find according to (39), (39′). In the rest the fragment of the full circle, connecting a pair of points, was divided into parts, passing separately by land and by sea. For each part, a finite difference grid was constructed with the number of points equal to the value $\left[2 + 0{,}25\sqrt{(\varphi_2 - \varphi_1)^2 + (\lambda_2 - \lambda_1)^2}\right]$, where $[\dots]$ is the function of the integer part of the number, and the pairs (φ_1, λ_1) and (φ_2, λ_2) denote the beginning and the end (in degrees) considered parts. In the future, in some cases, in order to save computing resources, parameter 0,25 was replaced by 0,125. As a result, for each pair of points from the total number $N \times (N-1)/2$, we compute transport integrals and find the mean values from each set.

Table 7 summarizes the computational experiment in a format where, randomly, according to the algorithm of Section V, $N = 320$ points were selected and the matrix D_{small} was calculated. The top line in the first row of Table 7 denotes the averaging operation. Taking into account the estimates from the preceding section, $g_1 \sim g_2 \sim 1, g_3 \sim g_4 \sim 10^{-3}$ it follows that each term in (32), (33) makes a comparable contribution from the point of view of the mean values. As a result, let us consider the choice of the values of the parameters $g_1 = g_2 = 1, g_3 = 10^{-3}, g_4 = 10^{-3}$.

Table 7. Average values of transport integrals

$\overline{\int_0^l \frac{dZ}{ds}\kappa(\frac{dZ}{ds})ds}$	$\overline{-\int_0^l \frac{dZ}{ds}\kappa(-\frac{dZ}{ds})ds}$	$\overline{\int_0^l \sqrt{1-(\frac{dZ}{ds})^2}ds}$	$\bar{l}$
$7{,}26 \cdot 10^{-4}$	$4{,}85 \cdot 10^{-4}$	0,7556	0,6383

According to the definition in (32), (33), and in Table 7, the integrals are taken along a path connecting a pair of points on the surface of the Earth. Since all the routes are located on one of the fragments of the complete circles, the transport integrals can be approximately considered proportional to the length of the arc. From this point of view, on the average, we can assume that the distance matrix D is the same as the distance matrix found for small fragments of complete circles, i.e. we assume further that $D = D_{\text{small}}$.

SECTION VIII.
THE TRANSPORT COST MINIMIZATION ALGORITHM

Let us return to the problem of transport costs optimizing in the form (34′), taking into account: 1) the features of the "land – sea" geometry and 2) the computational complexity of the transport cost functional Tr calculating and, in particular, its partial derivatives of variables $z_1, \dots, z_N$. Suppose that in the previous step of the iterative procedure, according to formulas (35′) the volumes of the habitat capacities are calculated, which allows to determine the transport costs functional (34′) within the current iteration.

To find the minimum of the function $Tr = Tr(\varphi_1, \dots, \varphi_N, \lambda_1, \dots, \lambda_N)$ we consider a slightly modified gradient descent scheme. Let us write the following system of ordinary differential equations:

$$\frac{d\varphi_i}{dt} = -b_i \text{sign}(\frac{\partial Tr}{\partial \varphi_i}), \frac{d\lambda_i}{dt} = -a_i \text{sign}(\frac{\partial Tr}{\partial \lambda_i}), i = 1, \dots, N, \qquad (40)$$

where t — some auxiliary argument, $\text{sign}(x) = 1$, $x > 0$; $\text{sign}(0) = 0$; $\text{sign}(x) = -1$, $x < 0$ — so-called "sign" function, and the sets of non-negative coefficients $\{a_1, \dots, a_N\}$ and $\{b_1, \dots, b_N\}$ are defined below.

We replace the ordinary derivatives in (40) by finite differences, then

$$\delta\varphi_i \cong -\delta t \cdot b_i \text{sign}(\frac{\partial Tr}{\partial \varphi_i}), \delta\lambda_i \cong -\delta t \cdot a_i \text{sign}(\frac{\partial Tr}{\partial \lambda_i}), \quad (41)$$

where $\delta\varphi_i, \delta\lambda_i, i = 1, \dots, N$ are the finite increments of functions, and δt is the final increment of the argument.

Taking into account (41), we write the transition algorithm from the current values of the functions $\{\varphi_1, \dots, \varphi_N, \lambda_1, \dots, \lambda_N\}$ with the value of the argument t to the new values of the functions $\{\varphi_1', \dots, \varphi_N', \lambda_1', \dots, \lambda_N'\}$ for the value of the argument $t + \delta t$, namely

$$\varphi_i' = \varphi_i - \delta t \cdot b_i \text{sign}(\frac{\partial Tr}{\partial \varphi_i}), \lambda_i' = \lambda_i - \delta t \cdot a_i \text{sign}(\frac{\partial Tr}{\partial \lambda_i}), \qquad (41')$$

where $i = 1, \dots, N$. If after recalculation, according to the algorithm (41′) one or more points are outside the land, we reduce the corresponding coefficients from the sets $\{a_1, \dots, a_N\}$ and $\{b_1, \dots, b_N\}$ so that the points return to the land. In case the coastline does not interfere with the movement of points, the corresponding coefficient values are assumed to be equal to one.

The value of the parameter δt in (41), (41′) was chosen from the set of steps $\delta t_m, \dots, \delta t_n$ of the form:

$$\delta t_m = \Xi/q^m, \delta t_{m+1} = \Xi/q^{m+1} \dots, \delta t_n = \Xi/q^n, \quad (42)$$

where $\Xi > 0$, $q > 1$ — some constants, and m, n ($m = 0, \dots, n;\ m \le n$) — natural numbers. Specific values of the parameters Ξ, q and n were chosen in the course of numerical calculations.

With allowance for (41′), (42), we calculate the new positions of the points $\{\varphi'_{k,1}, \dots, \varphi'_{k,N}, \lambda'_{k,1}, \dots, \lambda'_{k,N}\}$ by the formulas:

$$\varphi'_{k,i} = \varphi_i - \delta t_k \cdot b_i \text{sign}(\frac{\partial Tr}{\partial \varphi_i}), \lambda'_{k,i} = \lambda_i - \delta t_k \cdot a_i \text{sign}(\frac{\partial Tr}{\partial \lambda_i}), \qquad (43)$$

with steps $\delta t_k, k = m, \dots, n$, as well as the functional values of transport costs:

$$Tr'_k = Tr\left(\varphi'_{k,1}, \dots, \varphi'_{k,N}, \lambda'_{k,1}, \dots, \lambda'_{k,N}\right), k = m, \dots, n. \qquad (44)$$

Assume that in the set (44), when viewed from left to right, there is a number k_*, at which the transportation costs become smaller than those that took place in the previous step of the gradient descent scheme, i.e.

$$Tr_{k_*} < Tr(\varphi_1, \dots, \varphi_N, \lambda_1, \dots, \lambda_N), k_* = m, \dots, n. \qquad (45)$$

If inequality (45) is satisfied, for some k_* it is assumed that the gradient descent step is completed and the new positions of the points are considered equal:

$$\varphi'_1 = \varphi'_{k_*,1}, \dots, \varphi'_N = \varphi'_{k_*,N}, \lambda'_1 = \lambda'_{k_*,1}, \dots, \lambda'_N = \lambda'_{k_*,N}. \qquad (46)$$

If inequality (45) is not satisfied for all values of $k_* = m, \dots, n$, then this step of the gradient descent procedure is also considered complete and the new positions of the points are chosen equal to:

$$\varphi'_1 = \varphi'_{n,1}, \dots, \varphi'_N = \varphi'_{n,N}, \lambda'_1 = \lambda'_{n,1}, \dots, \lambda'_N = \lambda'_{n,N}. \quad (46')$$

To close the minimization algorithm (40) — (46′) it is necessary to clarify the procedure for counting the number m in the set (42). We denote the number k_* from the previous step of the procedure (41′) — (46′) with the symbol $\check{k}_*$, then the number m in the set (42) is calculated according to the formula: $m = \check{k}_* = 0$ and $m = \check{k}_* - 1, \check{k}_* > 0$.

According to the algorithm (40) — (46′), it is necessary to have partial derivatives of transport cost functions $Tr = Tr(\varphi_1, \dots, \varphi_N, \lambda_1, \dots, \lambda_N)$ on the coordinates of the points. Since it is difficult to do this analytically, it makes sense to consider the finite differences. We introduce some increments of the arguments $\Delta\varphi_i, \Delta\lambda_i, i = 1, \dots, N$ and write the following expressions:

$$P_i = Tr(\dots, \varphi_i + \Delta\varphi_i, \dots, \lambda), R_i = Tr(\varphi, \dots, \lambda_i + \Delta\lambda_i, \dots), \quad (47)$$

where $i = 1, \dots, N$. In this case, as above, we will assume that N points with coordinates $(\varphi_i + \Delta\varphi_i, \lambda_i + \Delta\lambda_i), i = 1, \dots, N$ are located within the land. If this is not the case, we vary the increments $\Delta\varphi_i, \Delta\lambda_i, i = 1, \dots, N$. Taking into account (47), we assume that

$$\frac{\partial Tr}{\partial \varphi_i} \cong \frac{P_i - Tr}{\Delta\varphi_i}, \frac{\partial Tr}{\partial \lambda_i} \cong \frac{R_i - Tr}{\Delta\lambda_i}. \qquad (48)$$

We perform the procedure of gradient descent (40) — (48) until the integral costs for traffic are reduced. If further decrease in traffic is not possible, we assume, according to formula (34′), that new positions of N points $z_i = (\varphi_i, \lambda_i), i = 1, \dots, N$ were found. We recalculate by the new values of N points the volumes of the capacities of the habitat $u_i, i = 1, \dots, N$ of the corresponding Voronoi polygons. We proceed to the next step, i.e. to the optimization procedure (40) — (48).

The inability to further reduce traffic means that the step of the gradient descent δt becomes minimal and equal to Ξ/q^n, and the proportion of the variation in the traffic costs for one gradient descent step periodically changes sign so that the integral costs for traffic fluctuate near a certain constant value.

In the procedure of gradient descent (40) — (48), in order to reduce the variability in the finite difference calculation of transport cost derivatives (47), (48), the relief was smoothed using the moving average procedure. The averaging was carried out over the nearest neighbours in the region of the square shape in the latitude-longitude coordinates with the number of points $7 \times 7 = 49$, while the original relief matrix had a resolution of $0{,}5^0$ and was represented in the form of a matrix 360×720.

For the initial estimate of the parameter β entering into the formulas (31′), (34), (34′), we will start with an approximate estimation of the share of transport costs in the world GDP in the range from 4% to 15%, depending on the development of the transport infrastructure. In the calculations, we will assume this share to be approximately 10%.

We estimate the parameter β, based on the formula (31′), assuming that the traffic costs is proportional to a some fraction ζ of the total capacity of the habitat, i.e.

$$Tr(\beta) = r \sum_{i=1}^{N} \left(1 - \frac{1}{\sum_{k=1}^{N} e^{-\beta d_{i,k}}}\right) u_i = \zeta \sum_{i=1}^{N} u_i. \qquad (49)$$

Considering the set: the constant r, the set $\{u_1, \dots, u_N\}$, matrix $\{d_{i,k}, i, k = 1, \dots, N\}$ and share ζ, we solve the equation (49) and find the coefficient β, which should provide at the final stage of the process of minimizing (34′), (35′) share of the traffic of the entire capacity of the habitat in the vicinity of 10%.

In Figure 19,a, according to (49), a typical example of the graph of the function $Tr = Tr(\beta)$ is constructed for $N = 36, r = 0{,}2$. The pentagram on the graph shows the value of the parameter $\beta = 2{,}7292 \cdot 10^3$, which was obtained by solving equation (49) at $\zeta = 0{,}11$. The distance matrix $D = \{d_{i,j}, i, j = 1, \dots, N\}$ was calculated from the random set of points

obtained according to the algorithm of Section V. Figure 19,b shows the positions of the random initial distribution of points (denoted by the centers of markers in the form of circles ○) on the Earth's surface, and also the corresponding Voronoi polygons.

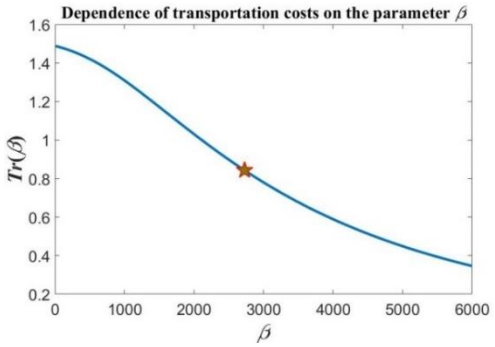

Figure 19,a. Dependence of transportation costs on the parameter β

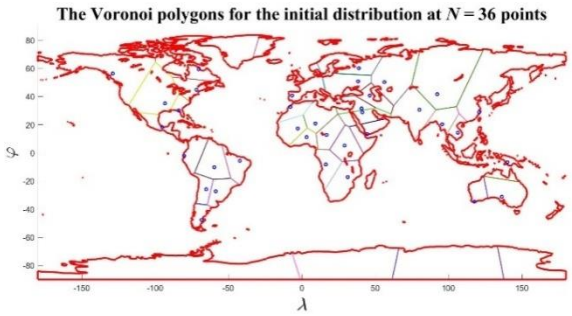

Figure 19,b. The Voronoi polygons for the initial distribution at $N = 36$ points

Figure 20,a,b shows the dynamics of the transport cost dependence on the gradient descent step number according to the procedure (40) — (48) with the parameters: $\Xi = 1$, $q = 4$, $n = 5$ for two sets of points by 36 and 72 respectively.

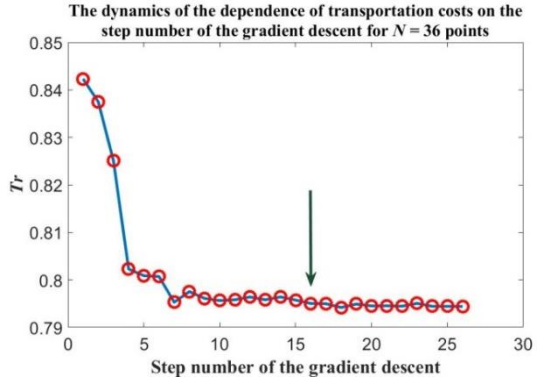

Figure 20,a. The dynamics of transport costs dependence on the step number of the gradient descent for $N = 36$ points

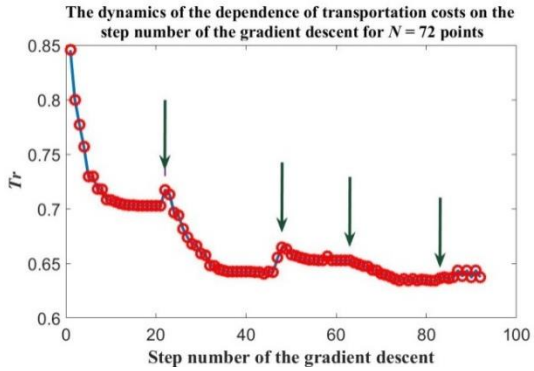

Figure 20,b. The dynamics of transport costs dependence on the step number of the gradient descent for $N = 72$ points

For 36 points in total, 26 steps of procedure (40) — (48) were implemented, while the cost of traffic decreased by 5,7% compared to the initial value. The circles in Figure 20,a,b indicate the transportation costs after each step of the gradient descent procedure. The total share of traffic costs for 36 points in relation to the entire capacity of the habitat was 10,4%. During the whole calculation, the set of capacities of the habitat $\{u_1, \dots, u_N\}$ was recounted once. In Figure 20,a,b place of the recount indicated by arrows. At the final stage of the calculations, Figure 20,a,b shows the output of the traffic values to a certain plateau.

Figure 21 shows the result of calculating the positions $N = 36$ points after applying the cost optimization procedure for transport (40) — (48) and one recalculation of the set of

habitats associated with each of the points. Initially, the points were chosen randomly according to the algorithm (21) — (24), they were marked by the center of the markers in the form of blue circles (○) in Figure 19,b and in Figure 21. After applying the optimization procedure (34′), (35′), (40) — (48) the position of the points is marked with markers in the form of pentagrams (★). The maxima of the displacements were $3{,}2^0$ and $3{,}4^0$ in latitude and longitude, respectively.

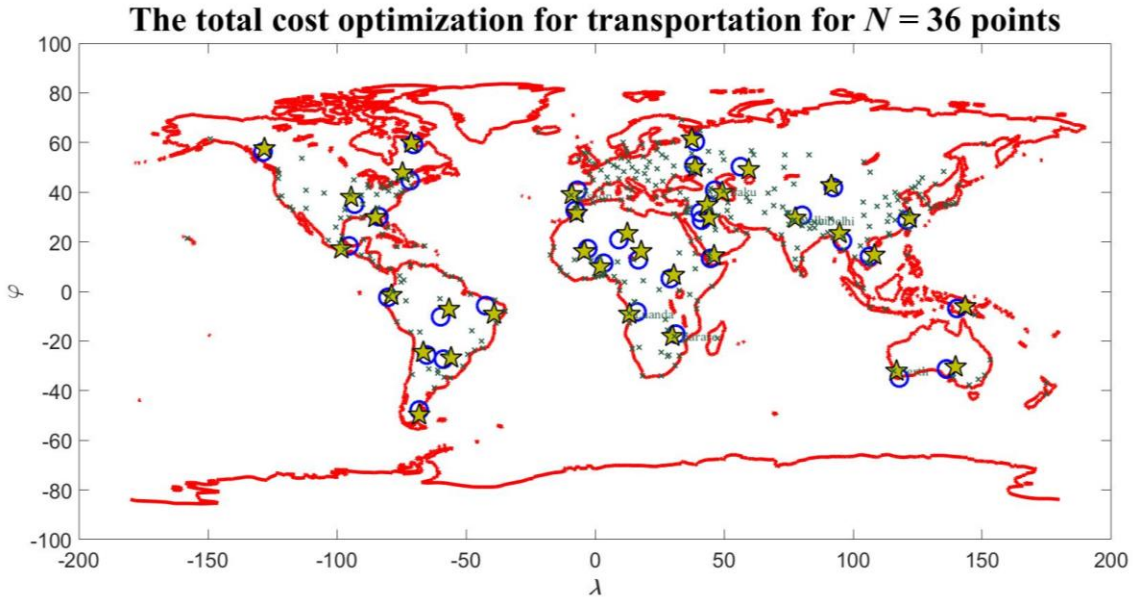

Figure 21. The result of optimization of transportation costs for $N = 36$ points, initially accidentally positioned on the surface of the Earth

On the map in Figure 21 with markers in the form of crosses (×) are marked the largest cities[3] on Earth in the number of 318. The names of 7 cities are noted, the coordinates of which were closest to the final positions $N = 36$ points. Taking into account (38) and (38′), the condition that the angular distance $D_{1,2}$ between a pair of points $z_1 = (\varphi_1, \lambda_1)$, $z_2 = (\varphi_2, \lambda_2)$ was less than one degree was chosen as a criterion for selecting cities, i.e. $D_{1,2} < 1^0$, where z_1 — coordinates of one of the cities from the set, and, and z_2 — one of the positions indicated by markers in the form of pentagrams.

The further testing of the algorithm for optimizing transportation costs (34′), (35′), (40) — (48) was carried out after doubling the number of points, i.e. for $N = 72$. Figure 20,b shows the dynamics of the dependence of transport costs on the step number of the gradient descent. In total, 88 steps of gradient descent (40) — (48) and four recalculations of the set of habitats were carried out according to the formula (35′). Other parameters of the procedure were the following values: $r = 0{,}2$; $\zeta = 0{,}11$; $\beta = 4{,}7711 \cdot 10^3$; $\Xi = 1$; $q = 4$; $n = 5$. After the optimization procedure, the traffic costs decreased by 24,6%, the share of traffic relative to the entire capacity of the habitat was 8,3%.

[3]The coordinates of the cities are taken from the database contained in the Matlab Mapping Toolbox.

Figure 22 shows the result of optimal positioning of $N = 72$ points. The initial positions of the points are denoted by markers in the form of blue circles (○), whose position centers are chosen randomly according to the algorithm (21) — (24). The final, optimal positions of the points are designated by markers in the form of pentagrams (★). The maximum variability of the positions of points in latitude and longitude did not exceed $12{,}3^0$ and $11{,}0^0$, respectively. The names of 10 cities are noted, the coordinates of which were within one angular degree to the total positions $N = 72$ points. On the map in Figure 22, the arrows connect the initial and final positions of points after the optimization procedure, the angular distance between which exceeds the value 3^0.

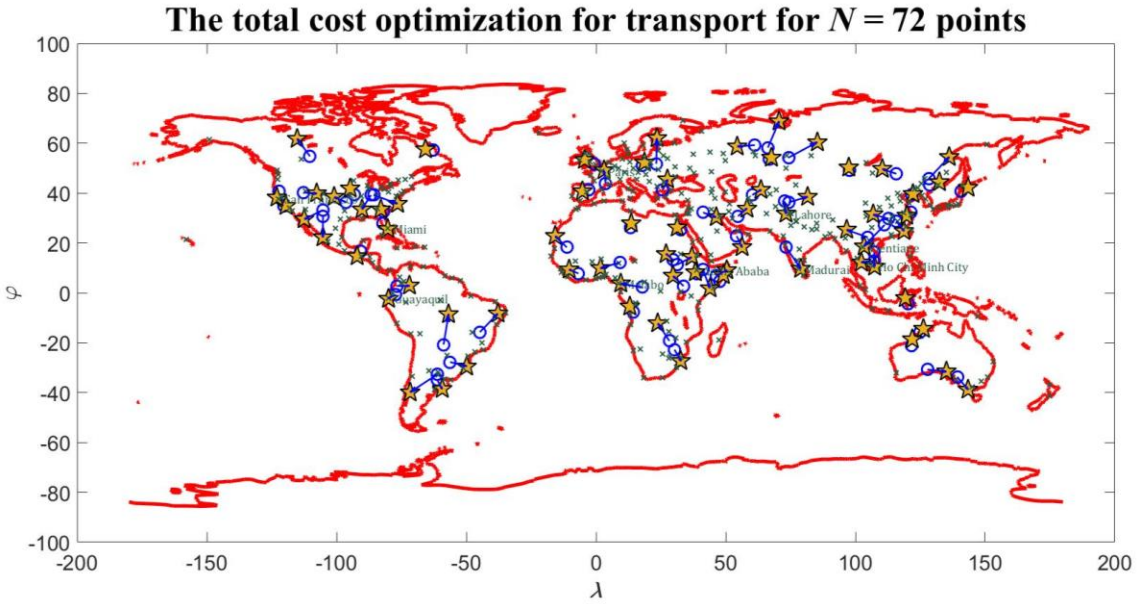

Figure 22. The result of optimization of transportation costs for $N = 72$ points, initially accidentally positioned on the surface of the Earth

Comparing Figure 21 and Figure 22, we can note the following. The optimal positions of the points (markers in the form of pentagrams) tend to fill the entire capacity of the habitat, that is, they tend to be distributed as uniformly as possible on the Earth's surface, taking into account the uneven density of the capacity of the habitat. Thus, the calculations of the optimal positioning of the points shown in Figure 21,22 confirm the realization of the minimax transport doctrine.

SECTION IX.
GEOPOLITICAL CLASSIFICATION OF POINTS AND TERRITORIES

Let us turn to the task of identifying the positioning of a set of points within the land in terms of marine or continental types. To do this, we define the percentage of "sea-continent" in global traffic, SeaContinent. Taking into account the formulas for the transport integrals (32), (33), we write the following relation:

$$\text{SeaContinent} = 100\% \frac{1}{1+\sum_{i,j=1}^{N} d_{\text{sea},i,j} / \sum_{i,j=1}^{N} d_{\text{earth},i,j}}, \quad (50)$$

where $d_{\text{sea},i,j}$ and $d_{\text{earth},i,j}$ are the parts of total distances, passing through the land and sea for a pair of points with indices i and j.

The percentage ratio (50) is normalized as follows. Let the sums of distances passing through the sea be zero, i.e. $d_{\text{sea},i,j} = 0, i, j = 1, \dots, N$, then the percentage ratio is 100%, i.e. SeaContinent = 100%. In this case, we can talk about a purely maritime type of traffic. From the point of view of transportation costs, the condition that the part of the generalized distance be equal to zero means that transportation costs on this section are absent.

In the case when the sums of distances passing over the land are zero, i.e. $d_{\text{earth},i,j} = 0, i, j = 1, \dots, N$, the percentage ratio is zero, i.e. SeaContinent = 0. In this case we are dealing with a purely continental type of traffic. Similar to the percentage ratio (50), normalized to the maritime traffic type, you can enter the percentage

$$\text{ContinentSea} = 100\% - \text{SeaContinent} = 100\% \frac{1}{1+\sum_{i,j=1}^{N} d_{\text{earth},i,j} / \sum_{i,j=1}^{N} d_{\text{sea},i,j}}, \quad (50')$$

normalized to continental type of traffic.

The percentage ratios (50), (50′) can be changed in two ways. First, by varying the parameters g_1, g_2, g_3, g_4, which characterize transport integrals (32), (33). Secondly, by varying the positions of points in relation to the traffic cost optimization procedure. The traffic optimization procedure was considered in the previous section.

We rewrite the percentage ratio (50) with an explicit selection of the parameters g_1, g_2, g_3, g_4. To do this, we introduce the notation for the four transport integrals, I_1, I_2, I_3, I_4, which appear in (32), (33), i.e.

$$I_1 = \int_0^l \frac{dZ}{ds} \kappa\left(\frac{dZ}{ds}\right) ds, \; I_2 = -\int_0^l \frac{dZ}{ds} \kappa\left(-\frac{dZ}{ds}\right) ds, \; I_3 = \int_0^l \sqrt{1 - \left(\frac{dZ}{ds}\right)^2} ds, \; I_4 = l. \quad (51)$$

Rewrite percentage (50) taking into account the transport integrals (51), then

$$\text{SeaContinent} = \frac{100\%}{1+g_4 \sum I_4/(g_1 \sum I_1+g_2 \sum I_2+g_3 \sum I_3)}, \qquad (52)$$

where $\sum I_k = \sum_{i,j=1}^{N} I_{k;i,j}$, $k = 1,2,3,4$, $I_{k;i,j}$ is the k-th transport integral between a pair of points i and j.

Table 8 shows the results of calculating the percentage ratio (50) for the number of points $N = 10$ and $N = 10^2$ respectively. In ten computational experiments, the points' positions were generated randomly according to the procedure of Section V.

Table 8. The results of calculating the percentage ratio of "sea – continent" for randomly positioned points, when $g_1 = 1$, $g_2 = 1$, $g_3 = 10^{-3}$, $g_4 = 10^{-3}$

SeaContinent	**#1**	**#2**	**#3**	**#4**	**#5**
$\textbf{SeaContinent}|_{N=10}$	89,9%	85,0%	63,0%	69,9%	73,9%
$\textbf{SeaContinent}|_{N=10^2}$	69,8%	68,7%	68,2%	69,0%	68,0%

From the analysis of the values of the percentage ratio according to Table 8 the following conclusions follow. First, with the selected values of the parameters g_1, g_2, g_3, g_4 we deal primarily with the sea traffic type (SeaContinent $> 63\%$). This is not surprising, because the surface of the Earth, as is known, is divided into land and sea in relation to 29,2% and 70,8% respectively. Secondly, even with the number of points exceeding $N = 10^2$, the variability of the percentage ratio is sharply reduced. This means that if you do not take into account the specially selected positioning geometry of points, then the percentage ratio can be significantly changed only due to the variation of parameters g_1, g_2, g_3, g_4.

In addition to Table 8, we consider the case when $N = 318$. As a set of points, let us consider the database of the 318 largest cities of the Earth, mentioned in the previous section. After calculating the percentage (50) for them with the parameters $g_1 = 1$, $g_2 = 1$, $g_3 = 10^{-3}$, $g_4 = 10^{-3}$ it turned out to be 73,17%. The obtained value is slightly higher than the current estimation of the share of sea transport in global traffic equal to 2/3. Change the parameter g_4 so as to ensure a percentage ratio of 2/3 or 66,67%. To do this, we express the parameter g_4 from equation (52) through three other parameter g_1, g_2, g_3, then

$$g_4 = \left(\frac{100\%}{\text{SeaContinent}} - 1\right)\left(\frac{\sum I_1}{\sum I_4} g_1 + \frac{\sum I_2}{\sum I_4} g_2 + \frac{\sum I_3}{\sum I_4} g_3\right). \qquad (53)$$

After substituting in (53) for the selected values $N = 318$ city points the SeaContinent $= 66{,}67\%$ value as well as the quantities found using the computational experiment: $\sum I_1 \cong 47{,}9151$; $\sum I_2 \cong 30{,}6374$; $\sum I_3 \cong 7{,}6271 \cdot 10^4$; $\sum I_4 \cong 5{,}6757 \cdot 10^4$, we obtain

$$g_4 = 0{,}5(8{,}4421 \cdot 10^{-4} g_1 + 5{,}3980 \cdot 10^{-4} g_2 + 1{,}3438 g_3). \qquad (53')$$

Substituting $g_1 = 1$, $g_2 = 1$, $g_3 = 10^{-3}$ into (53′), we find the modified value of the parameter $g_4 = 1{,}3639 \cdot 10^{-3}$, which provides a percentage ratio equal to 66,67% (before the procedure for minimization of transportation costs).

By analogy with (50), we construct a percentage ratio for each point from a certain set. Taking into account that the matrices $d_{\text{sea},i,j}$ and $d_{\text{earth},i,j}$, $i,j = 1,\dots,N$ are not symmetric in general, we will make the following percentage ratio:

$$\text{SeaContinent}_i = \frac{100\%}{1+\sum_{j=1}^{N}(d_{\text{sea},i,j}+d_{\text{sea},j,i})/\sum_{j=1}^{N}(d_{\text{earth},i,j}+d_{\text{earth},j,i})}, \qquad (54)$$

where $i = 1,\dots,N$. The percentage ratio (54) allows us to estimate the "sea – continent" relationship for each point from a given set.

Taking into account the definition in (54), we classify 318 points-cities in terms of preferences "sea – continent". After estimating the global percentage of 66,67% in (53), (53′) it became clear that this value acts as a preference separator in the "sea – continent" relation. In other words, if for some i-th point $\text{SeaContinent}_i > 66{,}67\%$, then this circumstance is interpreted in the sense that the i-th point is oriented to the sea. Conversely, if some i-th point is such that $\text{SeaContinent}_i < 66{,}67\%$, then this means that the i-th point is oriented to the continent. The word "orientation" is interpreted in the sense of a geopolitical confrontation, that is, the "sea" strives for power over the "continent" and, on the contrary, the "continent" is striving to acquire the "sea".

We note the following important circumstance in the matter of the confrontation between the sea and the continent. If some i-th point is focused on the sea, it means that it is rooted in the continent or, alternatively, is positioned continental. Conversely, if the i-th point is focused on the continent, it means that it is rooted in the sea, or, otherwise, has a maritime positioning. Thus, each point (the corresponding territory) has two attributes: 1) orientation and 2) positioning. From the point of view of geopolitics, both attributes with respect to each point have opposite names in terms of "sea – continent". This means that if there is a sea orientation, the positioning is continental and vice versa. The attribute "orientation" is characterized by a percentage ratio, SeaContinent; attribute "positioning" — the percentage ratio, ContinentSea. These verbal formulas should be understood in a metaphorical sense. All points having both a marine and continental type of orientation are ground-based.

Figure 23 shows the result of a computational experiment on the calculation of percentage ratios (54) for each of the 318 points-cities. When calculating transport integrals, the following parameter values were selected: $g_1 = 1$, $g_2 = 1$, $g_3 = 10^{-3}$, $g_4 = 1{,}3639 \cdot 10^{-3}$. Figure 23 shows a map-classification of 318 points-cities in terms of their orientation, either at the sea or on the continent. Points-cities are marked with markers in the form of pentagrams, surrounded by suitable polygons Voronoi. The cities and regions marked in brown are oriented to the continent.

According to the map in Figure 23, there is a huge cluster of regions marked in blue, which are oriented towards the sea. This cluster is called the "Continent", it consists of Europe, Asia, North and Equatorial Africa, and also from a small fragment in North America. The continent is surrounded by a multitude of scattered territories, which consist of almost the whole of North America, South America, South Africa, Australia, New Zealand and Oceania.

Antarctica should also be included in this group. All these regions are oriented to the continent, i.e. they have marine positioning. In this regard, let's name the whole set of territories that have a sea positioning “Sea”.

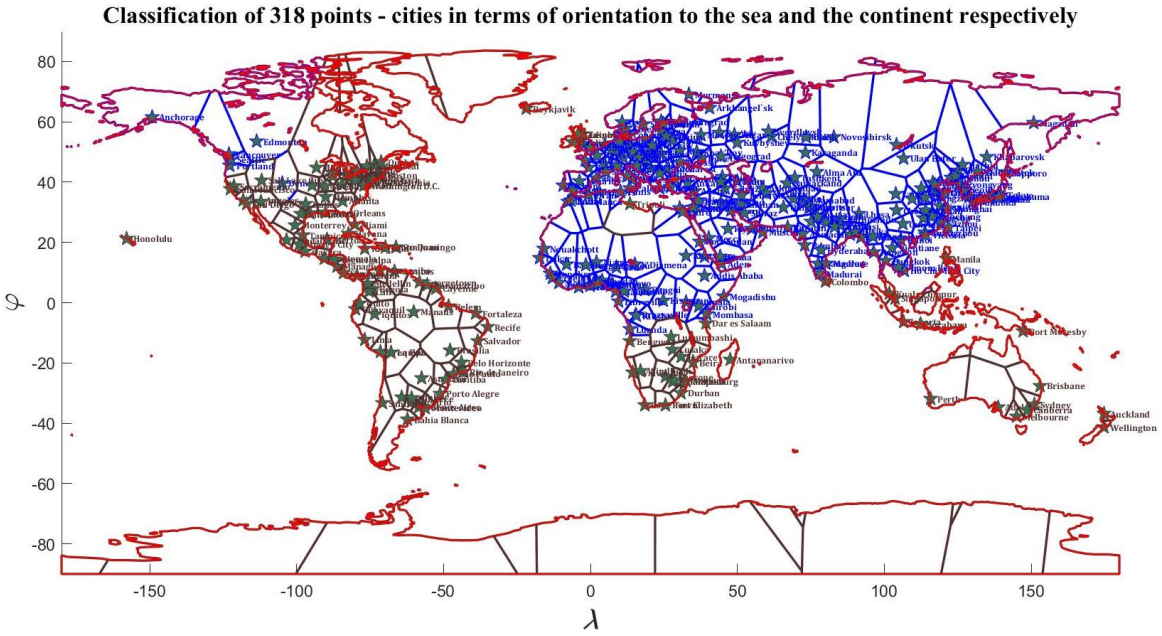

Figure 23. Classification of 318 points-cities in terms of orientation to the sea (blue) and to the continent (brown color) respectively

Figures 24,a,b show individual fragments of the map in Figure 23, in which two special cases of mixing territories with the opposite orientation are identified. Figure 24,a shows North America, in which all territories are oriented to the Continent except for six ones. These six territories include the territories associated with cities such as Anchorage (69,1%), Vancouver (67,8%), Seattle (67,5%), Portland (67,1%), Edmonton (69,3%) and Denver (67,9%).

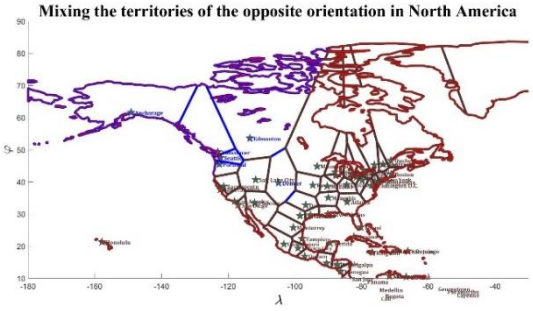

Figure 24,a. Mixing the territories of the opposite orientation in North America

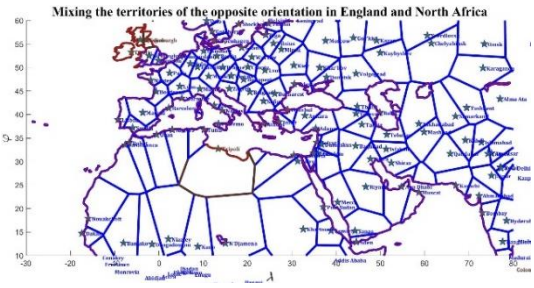

Figure 24,b. Mixing the territories of the opposite orientation in England and North Africa

Figure 24,b shows Europe and North Africa, in which all the territories are oriented to the sea except for four ones. These four territories include the territories associated with such

cities as Dublin (64,8%), Glasgow (64,8%), Edinburgh (64,6%) and Tripoli (66,66%). Percentage ratio 66,66% for Tripoli slightly less than the threshold value 66,67%, i.e. the area associated with Tripoli, is a border between two opposite orientations.

Note that all of the above orientations of the territories (at sea, on the continent) should be interpreted from the point of view of geopolitics. The verdict about this or that orientation of the city (territory) was obtained by calculating the percentage (54), which was compared with the global percentage ratio of 66,67%.

Let's compare the total capacity of the habitat area, oriented to the sea, U_{Sea}, with the total capacity of the habitat area, oriented to the continent, $U_{\text{Continent}}$. We calculate these values by the formulas:

$$U_{\text{Sea}} = \sum_{i=1,\text{SeaContinent}_i>66,67\%}^{318} u_i,\ U_{\text{Continent}} = \sum_{i=1,\text{SeaContinent}_i\leq 66,67\%}^{318} u_i, \qquad (55)$$

where $u_i, i = 1, \dots, 318$ — the habitat capacity of each of the 318 Voronoi polygons, whose appearance is shown in Figure 23,24. In the sums (55) only those terms whose percentage ratios satisfy the corresponding inequalities were taken into account.

After calculating the values of (55), it turned out that $100\%U_{\text{Sea}}/U = 51{,}73\%$, $100\%U_{\text{Continent}}/U = 48{,}27\%$, where U is the global capacity of the habitat. Thus, the potential for a geopolitical confrontation between territories oriented toward the sea and the continent is in the proportion of 51,73% to 48,27%, that is approximately equal.

We construct analogues of clusters of territories called “Heartland” and “Rimland”. These concepts are typical for classical geopolitics, they were introduced in the first half of the twentieth century by H.J. Mackinder [7] and N.J. Spykmen [12], respectively. We will also define the place where the notorious geographic “axis” of history passes.

According to Figure 23 continental positioned territories (corresponding Voronoi polygons) are determined from the condition that the individual percentage ratio is more of 66,67%. Let such territories be N_C. Let us find among these territories the average value of the percentage ratio C according to the following formula:

$$C = \frac{1}{N_C} \sum_{i=1,\text{SeaContinent}_i>66,67\%}^{318} \text{SeaContinent}_i. \qquad (56)$$

The presence of the average percentage ratio calculated according to (56) allows us to divide the territories into two categories, in which the individual percentages are in two ranges: $[66{,}67\%; C]$ and $[C; \max_{1\leq i\leq 318} \text{SeaContinent}_i]$. Territories falling within the first range we refer to Rimland, and within the second range — to Heartland.
As candidates for the geographical location of the “axis” of history, using the weighted average, we define two points. The weights will be the corresponding values of the capacities of the habitat of each of the territories.

The first point acts as a center of "gravity" for all territories oriented to the sea or continental-positioned. The position (φ_C, λ_C) of this point is found according to the formulas:

$$\varphi_C = \frac{\sum_{i=1,\text{SeaContinent}_i>66,67\%}^{318} \varphi_i u_i}{\sum_{i=1,\text{SeaContinent}_i>66,67\%}^{318} u_i}, \lambda_C = \frac{\sum_{i=1,\text{SeaContinent}_i>66,67\%}^{318} \lambda_i u_i}{\sum_{i=1,\text{SeaContinent}_i>66,67\%}^{318} u_i}. \quad (57)$$

The second point acts as the center of gravity for all territories attributed to Heartland. The position (φ_H, λ_H) of this point is found by formulas:

$$\varphi_H = \frac{\sum_{i=1,\text{SeaContinent}_i>C}^{318} \varphi_i u_i}{\sum_{i=1,\text{SeaContinent}_i>C}^{318} u_i}, \lambda_H = \frac{\sum_{i=1,\text{SeaContinent}_i>C}^{318} \lambda_i u_i}{\sum_{i=1,\text{SeaContinent}_i>C}^{318} u_i}. \quad (58)$$

In the framework of the above model considerations, we will construct a map with Rimland, Heartland and a pair of points (57), (58), applicants for the geographical "axis" of history. On Figure 25 the result is shown. Black colour is allocated to the territories attributed to Heartland, red colour is allocated to the territories attributed to Rimland.

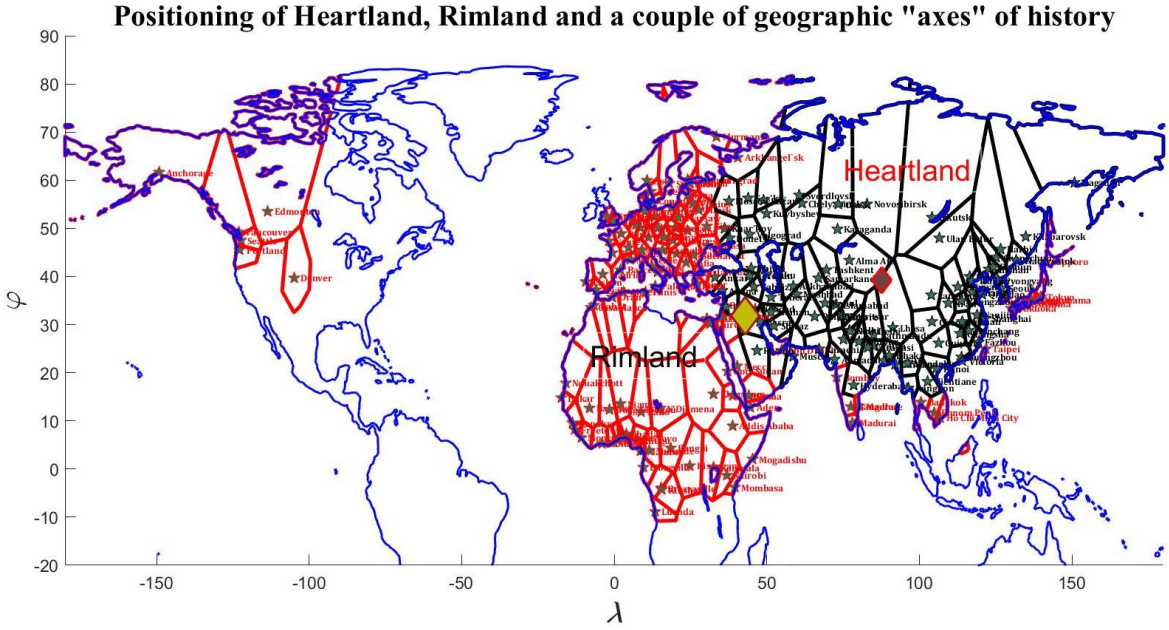

Figure 25. Positioning of Heartland, Rimland and a couple of geographic "axes" of history

It turned out that the division of territories into Rimland and Heartland is determined with the value of the percentage ratio equal to 73,7%, because $C = 73{,}7\%$. The Heartland has hit 83 of the territory, and in the Rimland — 119, total N_C=202. In terms of the capacity of the habitat, the shares of Heartland and Rimland in the Continent were 47,52% and 52,48% respectively.

Finally, two points representing the geographical "axis" of history were calculated and plotted on the map (two markers in the form of rhombuses). Larger rhombus indicates the point with coordinates $\varphi_C = 31{,}8386^0$, $\lambda_C = 42{,}9602^0$, which correspond to the city of Karbala in Iraq. Smaller rhombus denotes the coordinates $\varphi_H = 39{,}1497^0$, $\lambda_H = 87{,}7375^0$, which correspond to the nameless positions in the Xinjiang Uygur Autonomous region of China.

Due to the importance of the terms "Heartland" and "Rimland" from the point of view of geopolitics, we will define within Heartland and Rimland a subdivision into two groups of regions relative to the corresponding average values of percentage ratios. In other words, we divide Heartland into Heartland 1 and Heartland 2 and, similarly, Rimland to Rimland 1 and Rimland 2.

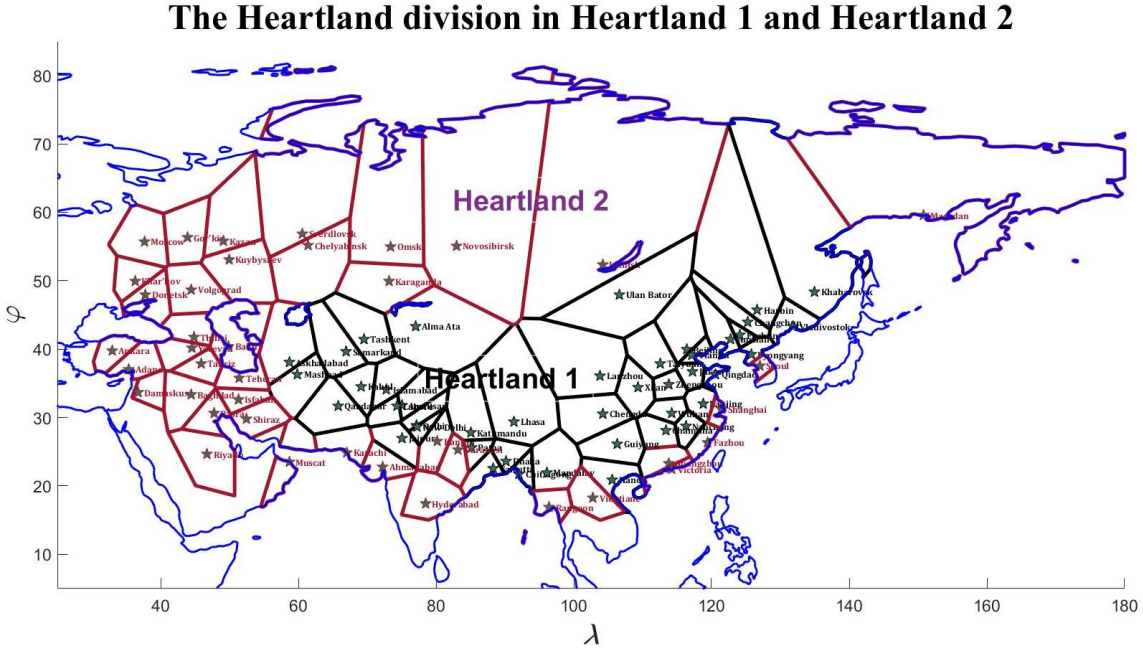

Figure 26. The Heartland division in Heartland 1 and Heartland 2

Figure 26 shows the map on which the desired subdivision into two Heartland is built, with Heartland 1 having a higher percentage ratio SeaContinent than Heartland 2. On the map, the boundaries of the territories classified as Heartland 1 are painted black, the boundaries of the territories classified as Heartland 2 are painted dark red.

The study of the map in Figure 26 leads to unexpected conclusions for classical geopolitics. Inside the Continent there is a compact core, called Heartland 1, which is surrounded by a belt called the Heartland 2. To Heartland 1 we can include Central Asia, Tibet, most of China, part of the Russian Federation.

Figure 27 shows the map on which the desired subdivision into two Rimlands is built, with Rimland 1 having a higher percentage ratio SeaContinent than Rimland 2. On the map, the

boundaries of the territories classified as Rimland 1 are painted red, the boundaries of the territories designated as Rimland 2 are colored magenta.

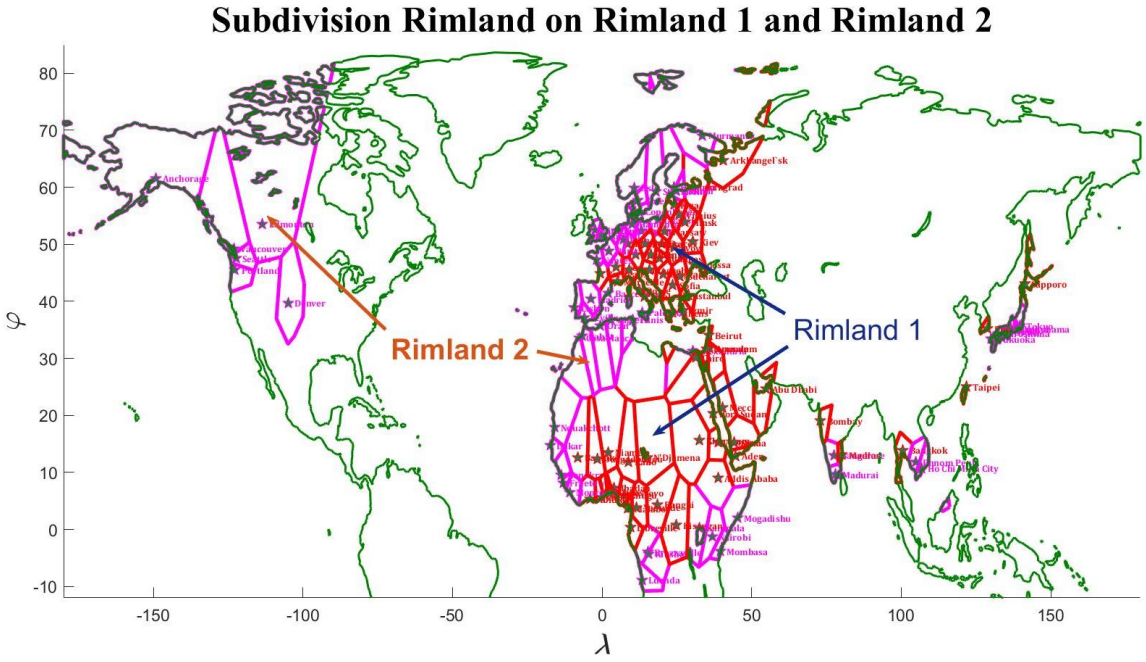

Figure 27. Subdivision Rimland on Rimland 1 and Rimland 2

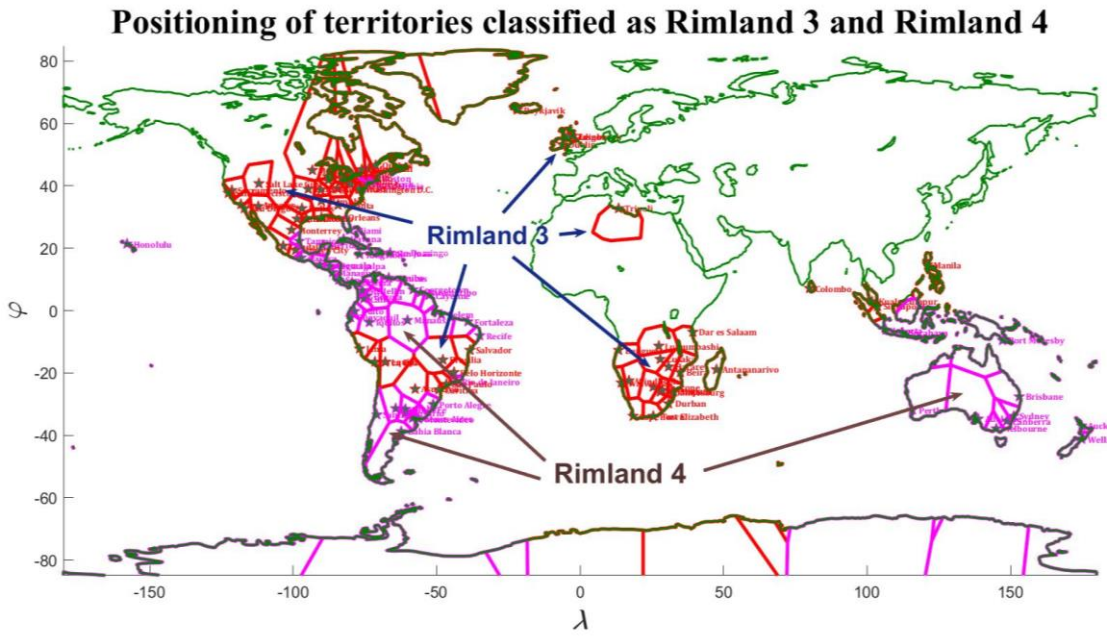

Figure 28. Positioning of territories classified as Rimland 3 and Rimland 4

The study of the map in Figure 27 shows a strong non-connectivity, both Rimland 1 and Rimland 2. In Rimland 1 reveals two large, compact clusters, is Central Europe and Central Africa.

It remains to examine in more detail the internal structure of territories oriented to the continent, i.e. positioned as marine ones. For these territories, the individual percentage ratio is less than or equal to 66,67%. We divide these territories into two classes with respect to the corresponding average value of the percentage ratios. Let's name these two classes of territories “Rimland 3” and “Rimland 4”. At the same time, the percentage ratios of the Rimland 3 territories are larger than the percentages of Rimland 4.

Figure 28 shows the map on which the desired division was built into two classes: Rimland 3 and Rimland 4. On the map, the borders of the territories classified as Rimland 3 are painted red, the boundaries of the territories referred to the Rimland 4 category are painted in magenta colour.

Attention is drawn to the map in Figure 28 attributing the USA, most of Canada, the middle part of South America, and also South Africa to Rimland 3. Finally, Central America, the south of South America, Australia and most of the Antarctic are parts of Rimland 4.

Figure 29,a. Positioning of a point and territory that has the maximum percentage ratio

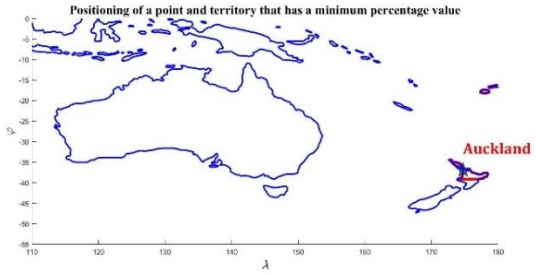

Figure 29,b. Positioning of a point and territory that has a minimum percentage value

We will find a couple of territories from our list that correspond to the maximum and minimum values of the percentage ratio. Figure 29 shows the result. Figure 29,a shows the city of Lanzhou and the corresponding territory, which have a maximum value of a percentage ratio equal to 82,84%. Figure 29,b shows the city of Auckland and the corresponding territory, which have a minimum percentage of 39,15%. The given cities and territories from the selected list are maximally removed from each other in the geopolitical sense of the word, with the city of Lanzhou located in Heartland 1 and the city of Oakland in Rimland 4.

Table 9. The final geopolitical classification of points and territories

Nomenclature of classes	Sea		Continent			
			Rimland		Heartland	
	Rimland 4	Rimland 3	Rimland 2	Rimland 1	Heartland 2	Heartland 1
SeaContinent, %	[39,15; 56,65]	[56,65; 66,67]	[66,67; 70,81]	[70,81; 73,74]	[73,74; 77,96]	[77,96; 82,84]
$U = 7{,}64$	1,5865	2,1010	0,9404	1,1339	0,9538	0,9244

Put together our classification of points and territories in terms of geopolitics. The result is presented in the form of a Table 9.

In Table 9 there is collected the nomenclature of 6 classes of points and territories, named in terms of geopolitics. The intervals of the values of the percentage ratio of points (territories) that characterize a particular class are given. The last line of Table 9 shows the capacities of the habitat of each class, as well as the sum of all individual capacities, equal to the global capacity of the habitat U.

Taking into account Table 9, we will build a map on which we will draw the geopolitical lines that separated Heartland 1, Heartland 2, Rimland 1, Rimland 2, Rimland 3, Rimland 4. In other words, we will construct a map representing the geopolitical structure of the Earth's surface according to this model. The result is shown in Figure 30.

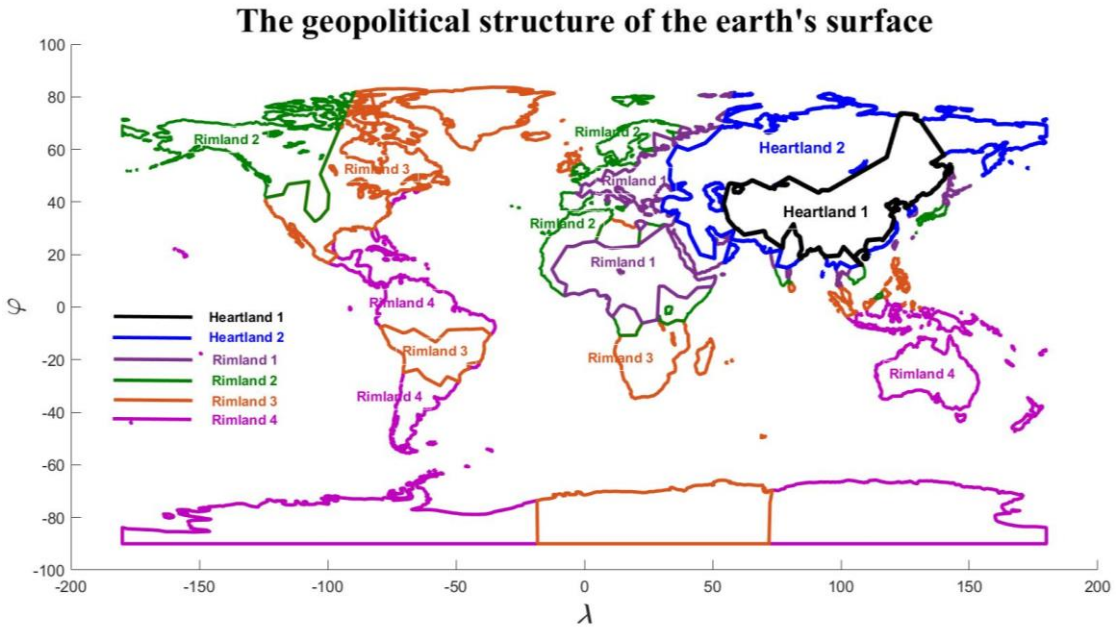

Figure 30. The geopolitical structure of the earth's surface

Compatible map of the geopolitical structure of the Earth, shown in Figure 30, with the current political map of the world. This will make it possible to build a list of States through whose territory certain geopolitical lines pass. These lines can be interpreted as “fracture” taking into account all the current and, perhaps, the past history of an individual state of the list. Since it is extremely difficult to combine all these lines on one map, we will consider some fragments of the global map.

Build a separate Heartland plus associated countries borders. Figure 31 shows the result. After studying this map, you can conclude the following. Russia is almost completely included in Heartland, more precisely in Heartland 2, there are only small intersections with Rimland. China is almost completely included in Hartland 1.

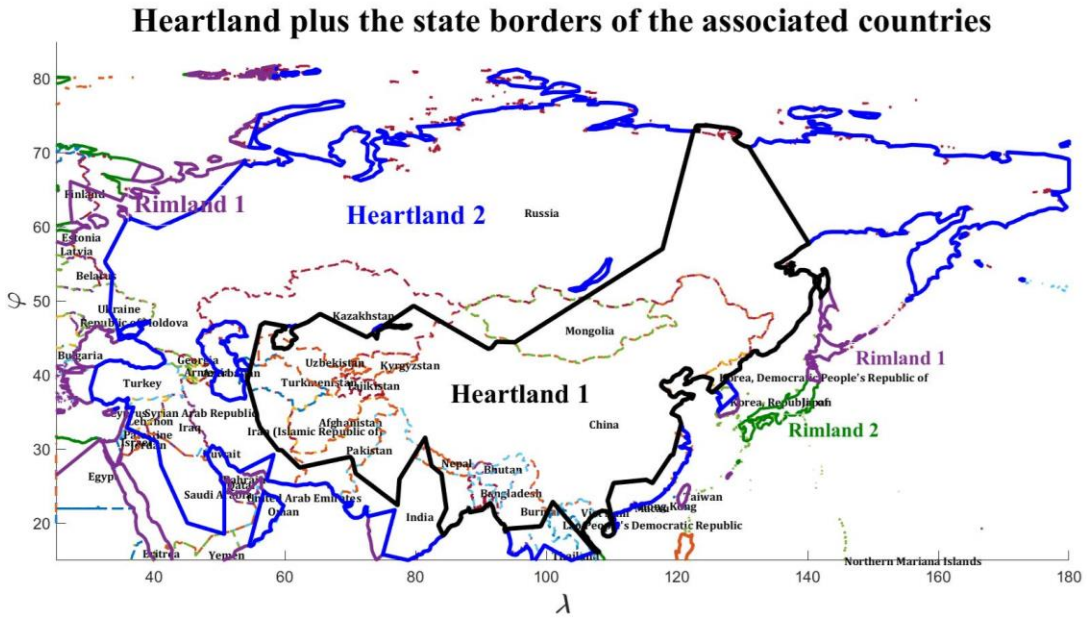

Figure 31. Heartland plus the state borders of the associated countries

A line dividing Rimland 1 and Heartland 2 passes through Ukraine from north to south. Taking into account current and past events in Ukraine, it can be concluded that the line dividing Rimland 1 and Heartland 2 is the line of the geopolitical fracture.

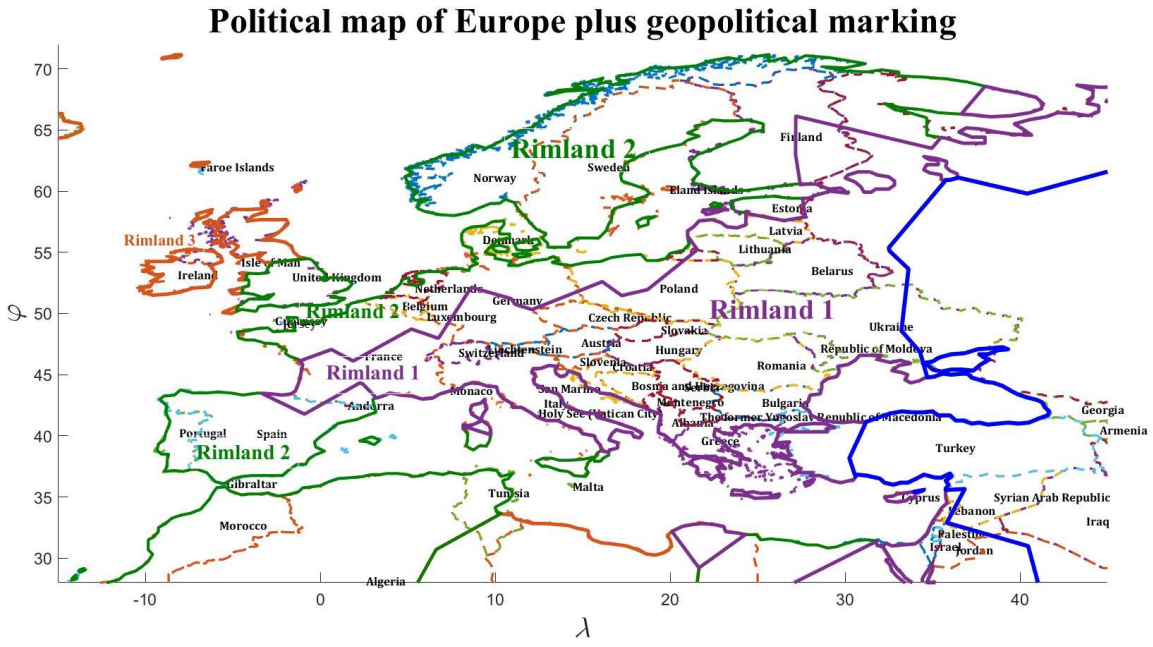

Figure 32. Political map of Europe plus geopolitical marking

It is interestingly that this same line crosses Turkey, and in Rimland 1 there is somewhere about a third of the territory of Turkey, and in Heartland 2 — two-thirds. This line passes through a part of Syria. It turns out that Oman belongs to Heartland 2. The same fracture

line passes through the territory of Thailand, cutting it almost in half. It turns out that Taiwan refers to Rimland 1. With the Korean peninsula, it is especially interestingly, two lines pass along it: the first line separates Heartland 1 from Heartland 2, the second line separates Heartland 2 from Rimland 1. Note that the first line is pretty close to the line dividing the two Koreas. Finally, it is rather interestingly, Japan almost in half to share the line separating Rimland 1 and Rimland 2. This line is not considered as a geopolitical fracture line.

Compatible political map of Europe and geopolitical lines defined on Figure 30. Figure 32 shows the desired map.

The visual inspection of the map in Figure 32 shows that within Europe there is a nucleus, called Rimland 1, surrounded by territories called Rimland 2. The line separating Rimland 1 and Rimland 2 most significantly crosses the territories of France, Germany, Poland and Finland. Finally, England is almost equally divided between Rimland 2 and Rimland 3.

In the terminology adopted above, we will continue to study the issue of the presence (absence) geopolitical fracture lines. Let's pay attention to Africa. Let us gather together the political map of Africa and draw geopolitical line, a list of which is shown in Figure 30. Figure 33 shows the final map for Africa.

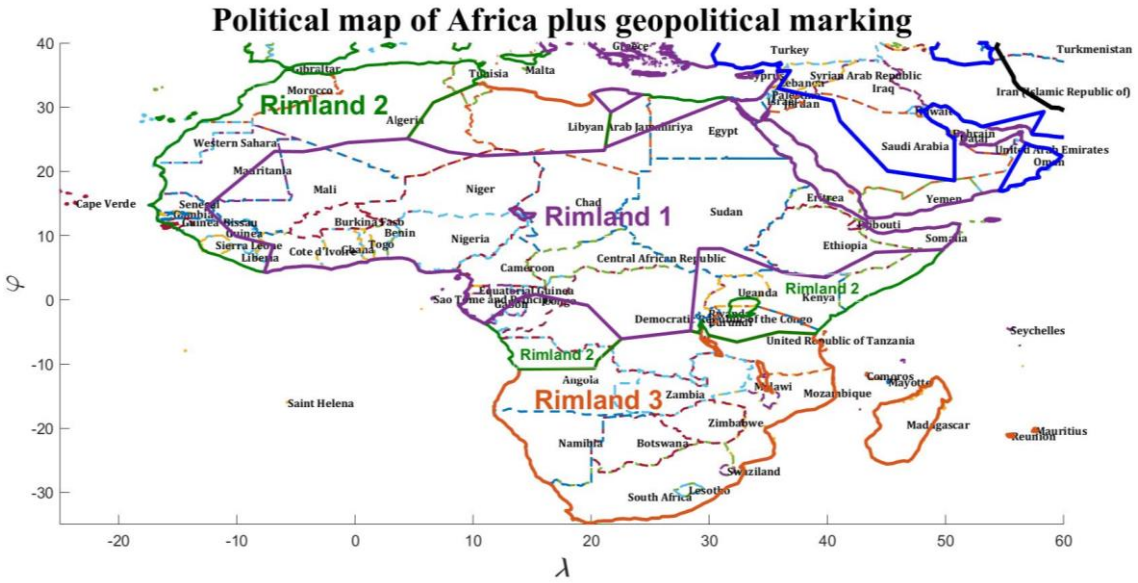

Figure 33. Political map of Africa plus geopolitical marking

The general examination of the map in Figure 33 shows that the State borders of individual countries on the African continent and geopolitical lines are not significantly coordinated. A more detailed study of the map shows the following. Somalia is divided in half by the lines separating Rimland 1 and Rimland 2. Given the past and current within Somali circumstances, we can consider the line separating Rimland 1 and Rimland 2 as a

geopolitical fracture. The Democratic Republic of the Congo, Algeria, the Libyan Arab Jamahiriya unite territories from three geopolitical classes: Rimland 1, Rimland 2 and Rimland 3. Through Gabon, Congo, Côte d'Ivoire, Guinea, Mauritania, Egypt, is the line separates Rimland 1 and Rimland 2, and through Angola — Rimland 2 and Rimland 3.

In connection with the analysis of the location of geopolitical lines in the North and South America (Figure 30), we note that there is no reason to consider them geopolitical fracture yet. If something negative in the geopolitical sense of the word will happen, so it is likely to be relevant to the line dividing Rimland 2 and Rimland 3 in northwest North America. The other geopolitical lines are not fracture, including because the neighbouring territories have a single marine positioning.

SECTION X.
THE RESULTS OF THE OPTIMIZATION OF TRANSPORT COSTS

Let us pass to the final task of the transport costs minimizing for the number of points equal to $N = 318$. As initial values for the 318 points, we choose the positions of the largest cities from the available database. Let us study the geometry of the optimal positioning of points within the land in the context of the "sea – continent" dichotomy. In this connection, we solve three problems of optimal positioning of points:

1) purely marine type of transportation of goods, when the cost of goods transportation by sea is zero, SeaContinent $= 100\%$;
2) purely continental type of transportation of goods, when the cost of transportation of goods by land is zero, SeaContinent $= 0\%$;
3) mixed type of transportation of goods, when the cost of transporting goods by sea and by land is comparable, for example, following (52) — (53′), we assume that SeaContinent $= 66{,}67\%$.

Note that, from the point of view of common sense, the first and second tasks are impossible in reality, since the transportation costs are minimized, but always remain non-zero for any type of transport. However, the solution of these problems is important for understanding the solution of the third problem in terms of the "sea – continent" dichotomy. According to (52), the condition for zeroing the transportation costs by sea is reduced to the condition $g_4 = 0$, similarly, zeroing the transportation costs by land is reduced to the conditions: $g_1 = g_2 = g_3 = 0$.

In order to present the solutions of the first and second tasks in general terms, it is necessary to take into account the minimax transport doctrine introduced earlier. Let the transport costs by the sea equal zero, in this case it is necessary to present the geographical map of the world without oceans, that is, only the land remains, within which, according to the minimax transport doctrine, the points are maximally removed from each other, taking into account the heterogeneity of the habitat density distribution. If transportation costs by land are equal to zero, it is necessary to present a geographical map of the world without continents, then for positioning of points there is only a coastline over which they are evenly distributed taking into account the heterogeneity of the habitat capacity density. Thus, the maritime type of transport communications promotes the movement of points into the continents and, conversely, the continental type of transport communications moves the points closer to the shoreline. The presented conclusions in a brief metaphorical form can be reduced to the formula of interpenetration of the sea and land: "sea $\rightleftarrows$ continent".

Let us solve the first problem, when it is considered that the goods transportation costs by sea are zero, i.e. SeaContinent $= 100\%$. Figure 34 shows the total optimization of 318 points in the first task. As the parameters for the optimization procedure discussed in Section IX, the following values were chosen: $r = 0{,}2$; $\zeta = 0{,}11$; $\beta = 1{,}7753 \cdot 10^4$; $\Xi = 1$; $q = 4$; $n = 5$, $g_1 = 1$, $g_2 = 1$, $g_3 = 10^{-3}$, $g_4 = 0$. Initially, the positions of the points

coincide with the positions of 318 cities. To achieve the optimum within the framework of this procedure, it took 30 steps and one recount of the habitat capacities for each of the points.

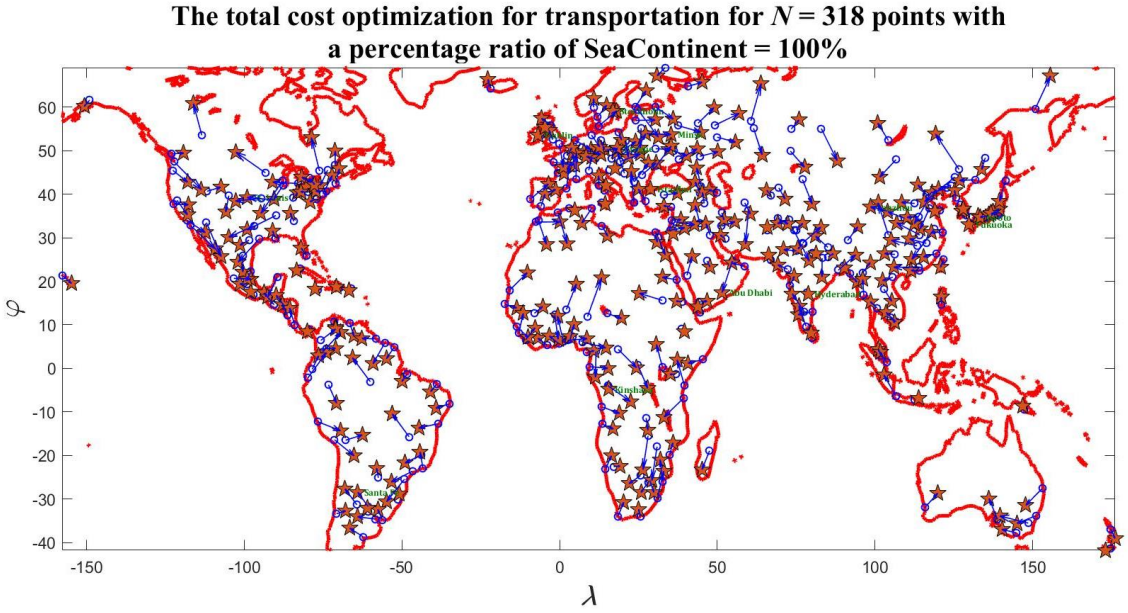

Figure 34. The total cost optimization for transportation for $N = 318$ points with a percentage ratio of SeaContinent $= 100\%$

In Figure 34, the centers of the markers in the form of blue circles (○) are the initial positions of the points. The centers of markers in the form of pentagrams (★) indicate the positions of points after transportation costs minimizing. As a result of the optimization procedure, the total transportation costs decreased by 39,6% and amounted to 6,6% of the total capacity of the habitat. In Figure 34, the names of cities marked the pentagrams in the number of 13, whose positions were within $0{,}5^0$ angular distance from one of the cities of the original list. The arrows indicate the transitions from the initial positions to the optimal ones when the angular distance exceeds the value $1{,}5^0$.

The study of the optimum positions of the points on Figure 34 demonstrates unambiguously the movement of points into the continents, which corresponds to the action of the minimax transport doctrine.

Let us proceed to the solution of the second problem, when it is assumed that the costs of transporting goods over land are zero, i.e. SeaContinent = 0%. Figure 35 shows the total optimization of 318 points in the second task. The following values were chosen as parameters of the optimization procedure: $r = 0{,}2$; $\zeta = 0{,}185$; $\beta = 2{,}5554 \cdot 10^4$; $\Xi = 1$; $q = 4$; $n = 5$, $g_1 = 0$, $g_2 = 0$, $g_3 = 0$, $g_4 = 10^{-3}$. Initially, the positions of the points coincided with the positions of 318 cities. To achieve the optimum within this procedure, it took 40 steps and three recalculations of the habitat capacities of each of the points.

In Figure 35, the centers of the markers in the form of blue circles (○) are the initial positions of the points. Centers of markers in the form of pentagrams (★) indicate the positions of points after the transportation costs minimizing. As a result of the optimization procedure, the total transportation costs decreased by 9,4% and amounted to 16,8% of the total capacity of the habitat. In Figure 35, the names of cities marked pentagrams in the number of 57, whose positions were within $0{,}5^0$ angular distance from one of the cities of the original list.

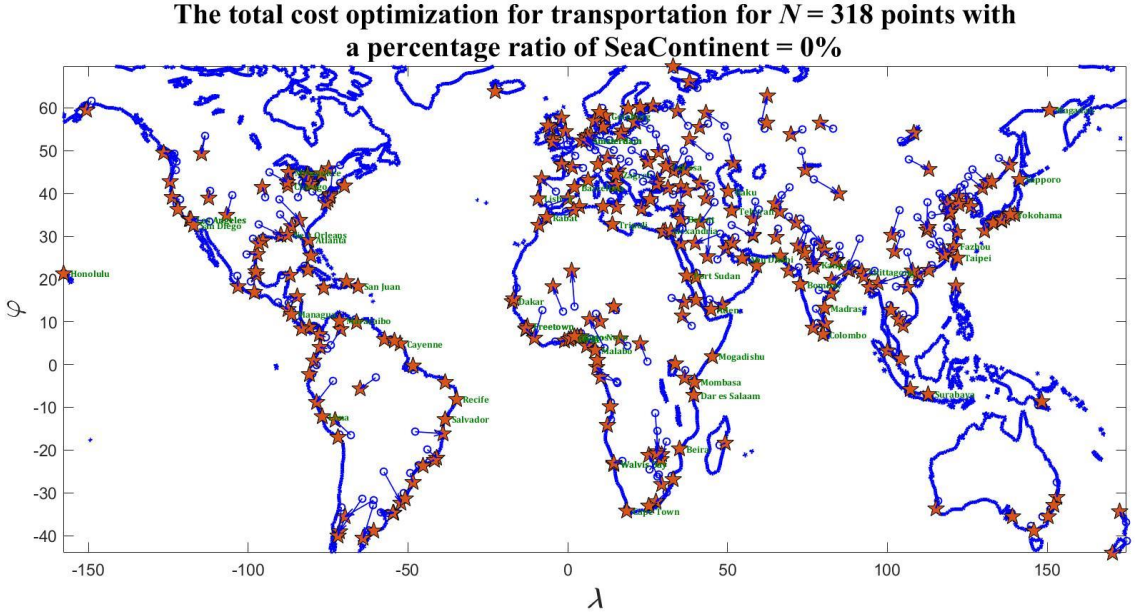

Figure 35. The total cost optimization for transportation for $N = 318$ points with a percentage ratio of SeaContinent $= 0\%$

The study of the optimum positions of the points in Figure 35 demonstrates the obvious movement of points closer to the shoreline in accordance with the action of the minimax transport doctrine for this case. Unfortunately, the available computational resources did not allow to use the optimization algorithm of the previous section with more advanced values of the parameters (N, Ξ, q, n), which would ensure the movement of all points to the shoreline.

In the context of the general description of the solutions of the first and second tasks, the meaning of the solution of the third problem, which has a direct relation to reality, becomes clear. In the case of non-zero transportation costs, both by sea and by land, the distribution of points is similar to something in between maritime and continental types of the positioning points of the first two tasks. As an example, consider the intermediate type, when the percentage ratio is chosen equal to SeaContinent = 66,67%, and the transport parameters according to (52) — (53′) — $g_1 = 1, g_2 = 1, g_3 = 10^{-3}, g_4 = 1{,}3639 \cdot 10^{-3}$.

Figure 36 shows the total transportation cost optimization for $N = 318$ points, the initial location of which coincided with the position of the largest cities from the existing

database. As parameters of the optimization procedure discussed in Section IX, the following values were chosen: $r = 0{,}2$; $\zeta = 0{,}11$; $\beta = 8{,}2564 \cdot 10^3$; $\Xi = 1$; $q = 4$; $n = 5$. To achieve the optimum within the framework of this procedure, 27 steps and two recalculations of the habitat capacities of each of the points were required. In Figure 36, the centers of the markers in the form of blue circles (○) are the initial positions of the points. Centers of markers in the form of pentagrams (★) indicate the positions of points after the transportation costs minimizing. As a result of the optimization procedure, the total transportation costs decreased by 7,8% and amounted to 10,1% of the total capacity of the habitat. In Figure 36, the names of cities marked pentagrams in the number of 31, whose positions were within $0{,}5^0$ angular distance from one of the cities of the original list.

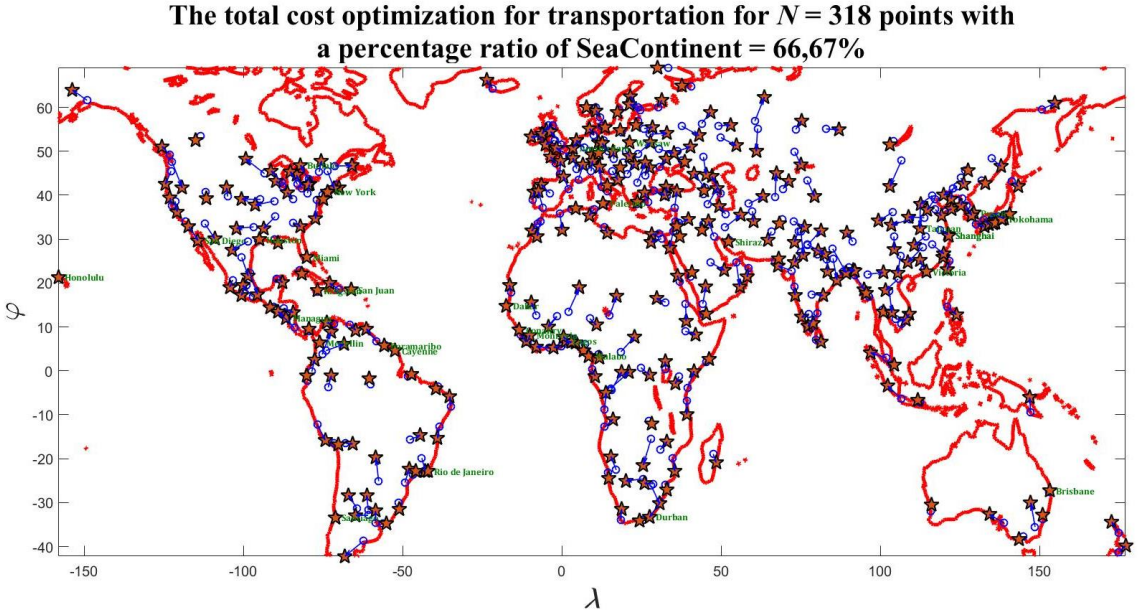

Figure 36. The total cost optimization for transportation for $N = 318$ points with a percentage ratio of SeaContinent $= 66,67\%$

As a result of solving the three problems of optimal transport positioning of a set of points mentioned above, we can formulate the following general problem. To choose the transport cost functional, so that the optimal positions of some set of points in relation to this functional correspond to the real positions of the cities acting as logistic centers. The computer resources available to the author at the current time are scant to solve this problem.

CONCLUSION

In this article we construct the mathematical model of geopolitics. The basis of the model is the central concept, called the “capacity of the habitat”. This concept is defined and calculated. The function of density of habitat capacity is constructed, which depends on the distribution of mean annual temperature and precipitation on the Earth's surface. A high correlation between the density of the capacity of the habitat and the population density of the Earth was established.

The density of habitat capacity has been calculated for each State. Among the record holders in the diminishing sequence were expected: Russia, the USA, Brazil, China, Australia, etc. An indicator has been determined and studied that has a specific habitat capacity per capita. The ranking of countries and territories by this indicator has been made. Particular attention is paid to the ratio of these indicators of individual countries in relation to the Russian Federation.

Studied the issue of the relationship of the density capacity of the habitat and topography was studied. The areas where 50% of the population and 50% of the habitat are concentrated are built and compared. The fields of the density gradient of the habitat are being constructed.

Classification of countries and territories is carried out in terms of “high – low” and “favorable – unfavorable”, i.e. in four categories, taking into account the relief and the density of the habitat. Maps of territories of all four types are constructed. An index of the diversity of individual territories and States is introduced and calculated.

An algorithm for random drawing of points on the surface of the land is developed, taking into account the density of the capacity of the habitat. This algorithm is necessary to develop a solution to the optimal positioning problem of points in terms of minimizing the transport costs between them.

A mathematical model of transport flows between individual points, which act as logistic nodes, is formulated. As the basis were used the well-known gravitational model and the exponential type of dependence on generalized distances between points. A minimax transport doctrine is introduced, which ensures, when optimizing the positions of the points, a minimum of transportation costs with a maximum of occupancy of the habitat taking into account the heterogeneous distribution of the density of the habitat capacity.

The method of calculating the generalized distances between points is described in detail, taking into account the difference in the sections passing over land and sea. These distances are estimated in terms of the specific energy costs for moving the weight unit of the conditioned cargo.

An algorithm for minimizing transport flows for an arbitrary set of points is constructed and tested. This algorithm is some modification of the gradient descent procedure taking

into account the shoreline and the non-connectivity of the domain of determining the positions of the points of the transport cost functional.

Within the calculation of global traffic, a special indicator has been constructed, called the percentage ratio “sea – continent”. Based on this indicator, the points (territories) are classified in geopolitical terms. This indicator allowed us to formalize the introduction of such well known in geopolitics concepts as Heartland and Rimland.

The division of Heartland into Heartland 1 and Heartland 2 was implemented. It turned out that the core of Hartland called Heartland 1 consists of Central Asia, Tibet, most of China and part of the Russian Federation. If Heartland and Rimland in geopolitics are usually referred to the “Continent”, then everything else is attributed to the “Sea”. It turned out that the capacities of the habitat of the territories positioned in the Sea and the Continent is about the same. The positioned in the Sea territories were divided into two groups with respect to the average value and named Rimland 3 and Rimland 4. The cities (Auckland and Lanzhou) are identified from the list under consideration, consisting of 318 cities, with minimum and maximum percentage ratios. A complete classification of all the city points and the corresponding areas from the adopted list in terms of geopolitics is carried out.

Combined global and regional maps containing political and geopolitical markings are constructed. The analysis of these maps for the presence of so-called geopolitical “fracture” is made. The presence of fracture can be said in the event that some geopolitical lines pass not along the border of an individual State, but through its territory, penetrating it deeply into it.

Within the framework of solving the minimizing transportation costs problem, 318 points were considered, the initial location of which coincided with the position of 318 largest cities on Earth. In a single complex, three subtasks were solved numerically. When solving each of the three subtasks, the minimax transport doctrine was essential. In the first subtask, it was assumed that the costs of transport by sea were zero; in the second task it was considered that the costs for transport by land were zero and, finally, in the third subtask, the real costs of transportation were chosen. It is shown that the optimal configuration of the points of the third subtask represents something in relation to the optimal configurations of the first two subtasks.

ACKNOWLEDGEMENTS

The author is grateful for help in translating article V.N. Nikolenko.

REFERENCES

1. Plokhotnikov, K.E. Normative model of global history. — Moscow: MSU Publishing House, 1996. 64p.
2. Plokhotnikov, K.E. Eschatological strategic initiative: historical, political, psychological, and mathematical reviews. – 2nd edition, reworked and enlarged. – Moscow: Hot line – Telecom, 2014. 251p.
3. http://climate.geog.udel.edu/~climate/html_pages/download.html#lw_temp2
4. http://climate.geog.udel.edu/~climate/html_pages/README.lw2.html
5. http://neo.sci.gsfc.nasa.gov/view.php?datasetId=SEDAC_POP
6. http://thematicmapping.org/downloads/world_borders.php
7. Mackinder, H.J. Democratic Ideals and Reality: A Study in the Politics of Reconstruction. Washington, DC: National Defence University Press, 1996.
8. Haushofer, K. An English Translation and Analysis of Major General Karl Ernst Haushofer's Geopolitics of the Pacific Ocean: Studies on the Relationship Between Geography and History. Edwin Mellen Press, 2002.
9. Walter, I. Location Theory and Trade Theory: Short-Run Analysis. Quarterly Journal of Economics 68, 2 (1954), 305–320.
10. Shvetsov, V.I. Mathematical modelling of traffic flows. Avtomat. & telemekh. 11 (2003) 3 — 46.
11. Zhinkin, V.B., Kachanov, I.V., Tovstyh, I.E. Theory of the ship. Vessel's fluid: a methodological guide for conducting practical exercises on the discipline “Theory of the ship”. — Minsk: BNTU, 2009.
12. Spykman, N.J., Geography and Foreign Policy, I, The American Political Science Review, 32, 1 (1938), 28-50.

Mathematical Model of Geopolitics

The mathematical model of geopolitics is a conditional name for several models, which are naturally connected and act as accompaniment to the main theme — geopolitics. All constructed work models made the transition to computing experiment, the results of which are given and discussed. The central concept of the mathematical model of geopolitics is introduced - the capacity of the habitat. Geopolitics is the climate, the relief, the logistics features of global commodity flows, the geopolitical confrontation in terms of the “sea-continent”, i.e. all that constitutes the material complex of living conditions of the inhabitants of the Earth. This complex, to a large extent, mediates the population's behavior from the political point of view. The author does not adhere to the position of natural determinism, which acts in the form of geopolitics, but tries to delineate the scope of the manifestation of geopolitics in real politics. The paper provides clarification and generalization of the generally accepted geopolitical classification of territories in terms of orientation and positioning either at sea or on the continent. The mathematical model of transport costs minimization for an arbitrary number of points acting in the form of logistic centers is formulated.

Konstantin Eduardovich Plokhotnikov

K.E. Plokhotnikov (psygma@yandex.ru) works at Lomonosov Moscow State University, Financial University under the Government of the Russian Federation. The author specializes in the development of mathematical models in natural and social sciences.

The mathematical model of geopolitics presented in the e-book follows from the previously developed by the author "Normative Model of Global History". The basic structural components of the normative model of global history are called geopatoms (GEOPolitical ATOMs). The task was to identify geopatoms in a global context. This mathematical model of geopolitics was built on this path.